Adapting A Time-Dependent Vaccination Game to Mask Compliance

by Sarah Smook

A Thesis
presented to
The University of Guelph

In partial fulfilment of requirements
for the degree of

Master of Science
in
Mathematics & Statistics

Guelph, Ontario, Canada

ABSTRACT

ADAPTING A TIME-DEPENDENT VACCINATION GAME TO MASK COMPLIANCE

Sarah Smook
University of Guelph, 2022

Advisor:
Dr. Monica-Gabriela Cojocaru

In this work, we provide a granular view of factors affecting COVID-19 disease transmission across Ontario, Canada and the 34 public health units composing it. Using multi-linear regression, we determine the perceived risk of infection and personal discomfort of complying with non-pharmaceutical interventions (NPIs). With the use of sequential quadratic programming, we solve our general nonlinear programming problem to obtain our Nash equilibrium and further, the expected NPI compliance rate across Ontario from March to December 2020. Using an SEIRL compartmental model, we compute the basic reproduction number for each PHU as well as the effective reproduction number using the expected NPI compliance determined. Finally, we explore the limitations of our work, discuss the success of our computations and highlight possible avenues of further refinement.

ACKNOWLEDGEMENTS

I would first like to thank my advisors, Dr. Monica Cojocaru and Dr. Ed Thommes for their expertise, guidance, feedback and support throughout this process. I am extraordinarily grateful to have had them care for and encourage me in my pursuit of my Master's degree.

I would additionally like to thank my research partners for their continual support and camaraderie throughout my masters. I thank my close friends and brother for the support and encouragement they provided during trying times.

Finally, I would like to thank my parents for their continual support throughout my academic journey. I am proud of the young woman you helped me become.

TABLE OF CONTENTS

LIST OF TABLES

LIST OF FIGURES

Chapter 1

Introduction

As the COVID-19 pandemic took over the world, the role of human behaviour in disease transmission became more apparent. With increasing case numbers, the government of Canada took to non-pharmaceutical interventions (NPIs) to mitigate the spread of COVID-19. While COVID posed many health threats on an individual scale, it put the medical system under immense stress. Hospitals around the globe were pushed to capacity and health care workers were placed in extreme work conditions. As the world worked collectively to find solutions to both short and long term issues, researchers amassed an abundant collection of data made readily available to use in further research. While we may never fully eradicate the virus that plagued the world since Spring 2020, researchers around the globe have collectively worked together to give us the tools and means to control disease spread and boost our immune response to such pathogens.

On January 25^{th}, 2020, the first positive case of the coronavirus was reported in Toronto, Ontario [8]. Due to rapid human-to-human transmission and intercontinental spread, the World Health Organization (WHO) declared SARS-CoV-2 virus a Public Health Emergency of International Concern (PHEIC) on January 30^{th}, 2020 [5]. While a majority of infected individuals were able to recover from the disease, those with compromised immune systems

were vulnerable to develop fatal complications. As of March 2022, there have been over 456 million confirmed cases of COVID-19 which included the 6.04 million deaths that resulted [6]. SARS-CoV-2 is related to SARS-CoV [63] and SARS-CoV-2 is a respiratory pathogen, thus airborne transmission occurs when inhaling respiratory droplets, however direct contact with contaminated surfaces are an additional means of transmission [26]. As this is a novel virus species, severe acute respiratory syndrome-related coronavirus, SARS-CoV-2 [40], pharmaceutical interventions were not available to the general population for a considerable amount of time. As mentioned by Harrison *et. al.* in their 2020 work, it is important to understand the transmission methods of the current COVID-19 pandemic so that public health authorities can make the most effective disease control measures including mask wearing, contact tracing and physical isolation [26].

While early 2021 brought about the vaccine rollout to all Canadians [8], in 2020 the only option we had to mitigate the spread of COVID-19 was through the use of NPIs. As SARS-CoV-2 is a respiratory pathogen, government officials implemented control measures such as physical distancing, lock-down periods, strong sanitation/disinfecting measures, increased ventilation, face mask and visor protection. [51].

SARS-COV-2 falls under the Betacoronavirus genus, which entails it to be a highly pathogenic RNA virus [26]. Every time the viral RNA is replicated, mistakes will occur, and not all of these mistakes are corrected; these mistakes are termed mutations [58]. As an RNA virus, SARS-COV-2 has a much higher mutation rate at about one mutation per each genome copy [58]. Once the virus is introduced to the body, the viral attachment protein is the mechanism through which the virus is able to invade host cells [26]. Through integration with the host cell DNA, mutation is an inevitable risk and these mutations can lead to new strains. As the virus propagates throughout the population, these random mutations can give way to new strains with higher transmission rates [58].

Despite the WHO's initial rejection of face mask usage in the general public, by January

30^{th}, the WHO published advice on the use of masks in community settings, highlighting the fact that face masks alone are not enough to provide an adequate level of protection required against SARS-CoV-2 pathogens [56]. As researchers worked tirelessly to develop a vaccine to protect the general population, governments across the globe had to take protective measures into their own hands. These measures led to the implementation of NPIs [21]. NPIs, are defined to be actions apart from being vaccinated and taking medication, that individuals and communities can take to mitigate the spread of illness [21]. Therefore it is crucial to care about compliance with NPIs is crucial to minimizing the spread thus decreasing transmission rates and thus minimizing mutations.

While several game theoretic mathematical modelling studies have been conducted that look to describe human behaviour with regard to vaccination [19, 14], the game theoretic framework is less explored in the context of modelling compliance with NPIs. In the past few years we have seen how dramatically and severely a disease can affect everyone around the world. When a disease is novel and there are no effective pharmaceutical protective methods available, the requirement for NPIs is apparent. Having the ability to predict individuals perceived risks and personal discomfort of complying with NPIs is the first step in providing public health officials with information how best to navigate disease mitigation in future. In this thesis we look to investigate and motivate the importance of looking at behavioural epidemiology on a more refined scale.

To obtain the refined view of Ontario's public health units, we must first determine the risk parameters of the general population. More specifically, we look to model the perceived risk of infection, which we denote $\bar{r}$ and the personal discomfort associated with complying to NPIs, $\tilde{r}$. We determine these values using multi-linear regression. Multi-linear regression is a statistical technique which uses various explanatory variables to predict the outcome of a response variable, thereby modelling the linear relationship between multiple variables [24]. We require the ratio of personal discomfort of NPI compliance to perceived risk of

infection, giving us $r = \frac{r}{\hat{r}}$. With this r value, we are able to simulate and compute the game of interest.

Game theory is defined as the study of mathematical models of conflict and cooperation between intelligent, rational decision-makers [36]. This provides general mathematical techniques to analyze situations in which two or more individuals make decisions that influence each others welfare [36]. To say a player is rational means they seek to optimize their objectives. Intelligent means a player looks for the optimal strategy in any given situation to achieve their optimum. Previous work has been done in which authors use game theory to study the dynamics of vaccination decisions in a population of distinct groups, where each group has differing perceptions of vaccine and infection risks [14]. Such models investigate the cumulative effect of the groups decisions on vaccine uptake. Since 1950 when John F. Nash first defined and characterized the notion of equilibrium in n-person games [38], there has been an abundance of research not only utilizing, but further enhancing the initial methodology. A Nash equilibrium is the most common way to define the solution of a non-cooperative game involving two or more players [44]. While Nash formulated and generalised the idea of non-cooperative behaviour in 1950 [38], we follow the reformulation done by Cojocaru *et. al.* [20] where the Nash game is reformulated as critical points of a system of differential equations, called a projected dynamical system (PDS) [20]. We note that the flow of a PDS remains in the constraint set of interest at all times, thus enabling an accurate description of how the system reaches a steady state and consequently how the players in a game adapt to reach a Nash equilibrium. Refer to Chapter 3 for more details and a full description of the model.

Within our model, we wish to determine the Nash equilibrium across each public health unit (PHU) from March 1^{st} to December 31^{st} 2020. To do so, we utilise MATLAB's general optimization solver SOLNP. SOLNP is a open sourced nonlinear optimization code written in Matlab by Yingyu Ye from Stanford University. SOLNP implements sequential quadratic

programming (SQP) to solve the linearly constrained problem [61]. SQP is an iterative procedure which models the non linear program for a given iterate $x^k, k \in \mathsf{N_0}$ using a quadratic programming subproblem which is then solved, giving a new iterate in the series x^{k+1} [50]. Ultimately this sequence $\{x^k\}_{k2\mathsf{N_0}}$ converges to a local minimum x , giving us the Nash equilibrium value we ultimately need for our game. Once we have x_{ij} where $i \in \{1, 2, \ldots, 34\}$ represents the 34 PHUs and $j \in \{1, 2, \ldots, 10\}$ represents the 10 months of interest over 2020, we are able to determine our expected NPI compliance values. Using this, we see the effect NPIs have at the more granular health unit scale through a comparative analysis of the effective reproduction number.

We introduce an SEIRL (Susceptible, Exposed, Infectious, Recovered and isoLated) model to investigate the effects of non-pharmaceutical measures on disease transmission and investigate the accuracy of our estimates when using the determined expected NPI compliance rate. SEIRL models follow the groundwork of SEIR (Susceptible, Exposed, Infectious, Recovered) models [15, 30] with the additional category of isolated individuals. As outlined in Chapter 4, movement occurs between each compartment of this model which gives us a system of ordinary differential equations. We look to determine the basic reproduction number R_0 across Ontario's 34 public health units as well as the effective reproduction number R_{eff}. We estimate these values using classic next generation matrix analysis [54] as well as with the use of known repositories of incidence data for Canada [3]. We define the reproduction number of an infectious disease (R_0) to represent the expected number of new cases produced by a single infectious individual in a fully susceptible population. In epidemiology, a pandemic is controllable and transmission numbers will die out when $R_0 < 1$. While estimating the basic reproduction number for COVID-19 proved to be challenging as it was dependent upon behavioural activity in local populations, the reported values for R_0 ranged from 2.2 to 6.49 both in China and overseas [31]. While whole populations start in this susceptible category, the progression of a pandemic decreases the number of susceptible

individuals in a given region as they move to another compartment within the model or out of the model. In doing so, the average number of secondary cases per infection changed as the population recovered by becoming immunized or dying. Consequently, as the pandemic progressed, these R_0 values gave rise to the effective reproduction number or R_{eff} which measures the average number of secondary cases per infection in a population at a given time [34].

1.1 Data Sources

Within this thesis, we use various sources of publicly-available data. We highlight how we use the information as well as where the reader can find this information. First, we access our incidence data through the Ontario case Data Catalogue [1]. Additionally, we access our hospitalizations data for Ontario Ontario hospitalizations Data Catalogue [2]. We utilise Oxford's COVID-19 Government Response Tracker Stringency index across Ontario to help determine a players personal discomfort to complying with NPIs. Google mobility data for each region of interest was retrieved from Google COVID-19 Community Mobility Reports. Finally, we obtained our mask compliance data from the Institute for Health Metrics and Evaluation. Using all of these sources, we compute our perceived risk of infection $\bar{r}$ and personal discomfort with NPI $\tilde{r}$ as well as our basic reproduction numbers. When we wish to look at the correlation between other variables and our determined values $(\bar{r}, \tilde{r}, R_0)$, we use public health unit level data from the 2016 Canadian census, from the Health Regions tab under the sub-provincial geography levels [7]. In the table below, we present the various values of the characteristics used in our correlation analysis.

PHU	Population Density ($/km^2$)	Median Income	Median Age	Proportion with Post Secondary
ALG	2.7	31719	49.1	0.42
BRN	119.5	33256	41.7	0.39
CHK	41.3	30895	45.8	0.37
DUR	255.9	37755	40.2	0.44
EOH	38.2	34166	45.8	0.39
GBC	18.8	32204	49	0.42
HAL	568.9	42577	40.5	0.5
HAM	480.6	32917	41.5	0.42
HDN	38.4	33277	46.5	0.38
HKP	19.8	32671	52	0.42
HPE	22.5	30592	47.8	0.4
HPH	17.4	33752	44.1	0.85
KFL	29.2	35298	44.5	0.46
LAM	42.2	34668	46.1	0.45
LGL	26.4	34940	48.9	0.44
MID	137.3	33533	40.3	0.45
NIA	241.5	31601	45.7	0.42
NPS	7.3	31279	48.3	0.44
NWR	0.4	33980	40.8	0.35
OTT	334.8	41857	40.1	0.52
OXF	47.3	33427	42.4	0.36
PEL	1108.1	30715	38.1	0.44
PQP	0.3	34436	42.4	0.37
PTC	35.9	31792	46.9	0.45
REN	6.9	34237	45	0.4
SMD	61.4	33890	44	0.41
SUD	4.2	36548	44.5	0.44
THB	0.7	35198	44.1	0.42
TOR	4334.4	30089	39.3	0.5
TSK	2.3	30937	47.3	0.39
WAT	390.9	35714	38.5	0.42
WDG	68.6	37882	40.4	0.42
WEC	215.5	33040	42.4	0.41
YRK	629.9	32994	41.1	0.47

Table 1.1: Variables of interest for correlation analyses taken from [7].

Chapter 2

Determining Risk Parameters

2.1 Constructing Risk Parameters

In this chapter we present the determination and computation of the perceived discomfort with NPIs and fear of infection under noncompliance, all within average individuals of each of the 34 public health regions in Ontario.

Using multi-linear regression analysis, we determine our perceived risk and discomfort estimates for each Public Health Unit. In Ontario, a PHU is defined as an official health agency established by a group of urban and rural municipalities to provide communities with more efficient health care programs [12]. Ontario is comprised of 34 public health units (PHUs) which are spread across the province. For our behavioural game discussed in Chapter 3, we require the perceived risk of infection $\bar{r}_i \ \forall \ i \in \{1, \ldots, 34\}$ and perceived personal discomfort $\tilde{r}_i \ \forall \ i \in \{1, \ldots, 34\}$ where i indexes the 34 PHUs in Ontario. We use multi-linear regression (MLR) to study the relationship between a dependent variable and multiple independent variables [48]. It is required that the dependent variable be continuous while the independent variables may be binary, categorical or continuous [48]. In general, a

Dependent (Y) Variables	Independent (X) Variables
Mask Compliance Google Mobility	Daily Case Data at the PHU level Daily Deaths at the PHU level Provincial Hospitalizations Ontario's Oxford stringency index

Table 2.1: Dependent and independent variables in our regression analysis

multi-linear regression model can be described as follows

$$Y = a + b_1 \times X_1 + b_2 \times X_2 + \cdots + b_n \times X_n$$

where Y is the dependent variables, $X_i, i \in \{1, \ldots, n\}$ are the independent variables with regression coefficients $b_i, i \in \{1, \ldots, n\}$ and a is the y-intercept. Refer to Table 2.1 to see what the independent and dependent variables are for our work.

2.1.1 Daily Case and Death Data

Using PHU level case data, we determined the total number of daily cases and deaths for each health unit. Ontario is the only province in Canada and one of the few authorities in the world which publishes daily COVID-19 case data based upon date of specimen collection [49]. This is an important distinction when using social mobility data as relying exclusively on daily data constructed on the basis of confirmation of test results could lead to misleading estimates if there are significant and inconsistent delays in the release of test confirmations [49]. Using these results, we determined the change in case numbers on a daily basis. If daily case numbers are greater than what they were the day before, we assign a value of 1, if case numbers decrease, we assign a value of 0 and if cases stay the same, we assign a value of 0.5. We follow the same procedure for determining daily deaths. We use these scaled results in the determination of $\tilde{r}$ as the personal discomfort of complying with NPIs depends less so upon the magnitude of the change in case numbers but rather the relative change in

direction. This is logical as news reports would often cite not only the number of cases in a region but also highlight whether they went up or down [8, 42].

2.1.2 Hospitalizations

For hospitalizations, we look at the provincial level rather than the regions by which the hospitals are aggregated (North, central, South, etc.). As we are trying to determine the perceived relative risk of infection, we follow what news was available to the general population throughout 2020. This would be major publications such as CTV news Toronto [8], and its affiliates in other cities across Ontario, as well as the direct news outlet for the Ontario provincial government, the Ontario News room. These major resources for Ontario residents looked at hospitalizations and Intensive Care Unit (ICU) cases at the provincial level. Hence we make the generalization that most players in our game will determine their perceived risk of infection depending upon the number of Ontario hospitalizations. More specifically, in our regression problem, each players perceived risk of infection is dependent upon the number of ICU cases. ICU cases were used instead of number of hospitalizations due to COVID-19 since although initially the media highlighted the number of hospitalized individuals, this soon transitioned to highlight the overwhelming number of cases that required intensive care. These severe cases alongside the less severe hospitalizations, took a heavy toll on hospitals and strained healthcare professionals across the province. Consequently, daily reports were given to the population through these media outlets, highlighting the deadly consequences the disease can have [8]. Thus when players in a given region are evaluating their perceived risk of infection, they are presented with information showcasing how severe health implications of coronavirus can be through ICU cases.

2.1.3 Oxford Stringency Index

When looking at how nations respond to the COVID-19 pandemic, we tend to discuss policy measures enacted by the government. These measures were put into place to help mitigate the spread and protect the community from this highly transmissible SARS-CoV-2 virus. The Oxford Covid-19 Government Response Tracker (OxCGRT) collects systematic information on the policy measures taken by governments. The various policy responses recorded by the OxCGRT were split into four indices that aggregate the data into a single number between 0 (no restrictions) and 100 (maximum restrictions). Each index uses relevant indicators which a government has acted upon and to what degree. Specifically, the OxCGRT tracks individual policy measures across 23 indicators and calculates several indices to provide an overview of government activity. These indices are calculated by taking the component-wise average of the individual factors that compose one index, as in Equation (2.1), k is the number of component indicators for an index and I_j is the sub-index score [25].

$$index = \frac{1}{k} \sum_{j=1}^{k} I_j \tag{2.1}$$

While the OxCGRT has a number of indices, this work makes use of the Stringency index. This index measures the strictness of "lockdown" policies that primarily restrict people's behaviour. As Canada falls under OxCGRT's primary datasets, they include some sub-national data which means in our research we use the OxCGRT Stringency index for Ontario. While this data cannot provide us with specific stringency imposed by local governments, it is appropriate to use this provincial scale in our work. Ontario residents may recall the"COVID-19 Response Framework: Keeping Ontario Safe and Open" which was introduced in November 2020. This article detailed a plan to reopen regions of Ontario by PHU according to what their current level was within this framework. These measures were split into 5 different categories, each of which consisted of varying degrees of preventative

and lockdown measures. In about 3-4 week periods, different regions loosened restrictions while others stayed in a full lockdown (see [9, 39]). While on paper this was a good idea, there were very few ways to regulate travel between these regions and thus regions would hop in and out of these lockdown periods. As of December 21, 2020 Ontario announced a province wide shutdown as case counts and hospitalizations began to exponentially increase once again [41]. As case numbers began to decrease in February of 2021, the Ontario government loosened measures following the same colour-coded framework only to be met with more cases which lead to yet another province-wide emergency stay at home order [42]. It was then in May 2021 that the government of Ontario announced their plan to restructure their road map to reopening the province which detailed a gradual, province-wide reopening plan incorporating vaccinations which had since become available. Rather than reopening the province by public health units, changes were implemented province-wide [43]. While there were changes made on a smaller scale, the government always reverted back to some "provincial standard" measure or lockdown. Therefore using the Oxford stringency index at this sub-level is appropriate as restrictions were essentially made on a provincial scale.

When looking at what specifically composes the Stringency index, there are nine indices as defined in Table 2.2. Note that C refers to *containment and closure policies* and H refers to *health system policies* [45]. Most of these indices have a binary flag variable which denotes whether they are "targeted" to a specific graphical region (flag $= 0$) or if there are a "general" policy which is applied across the whole country.

In Appendix A we discuss an other stringency index that is tailored more to the Canadian landscape and economic climate. We note that while this index is meant to be better suited to what happened in Canada, it does not provide a more granular view of stringency measures enforced to the general population. Thus we use the Oxford stringency index mentioned above.

ID	Name	Description	Measurement	Coding
$C1$	$C1$_School closing	Record closings of schools and universities	Ordinal scale	0 - no measures 1 - recommend closing or all schools open with alterations resulting in significant differences compared to non-Covid-19 operations 2 - require closing (only some levels or categories, eg just high school, or just public schools) 3 - require closing all levels Blank - no data
$C2$	$C2$_Workplace closing	Record closings of workplaces	Ordinal scale	0 - no measures 1 - recommend closing (or recommend work from home) or all businesses open with alterations resulting in significant differences compared to non-Covid-19 operation 2 - require closing (or work from home) for some sectors or categories of workers 3 - require closing (or work from home) for all-but-essential workplaces (eg grocery stores, doctors) Blank - no data
$C3$	$C3$_Cancel public events	Record cancelling public events	Ordinal scale	0 - no measures 1 - recommend cancelling 2 - require cancelling Blank - no data
$C4$	$C4$_Restrictions on gatherings	Record limits on gatherings	Ordinal scale	0 - no restrictions 1 - restrictions on very large gatherings (the limit is above 1000 people) 2 - restrictions on gatherings between 101-1000 people 3 - restrictions on gatherings between 11-100 people 4 - restrictions on gatherings of 10 people or less Blank - no data
$C5$	$C5$_Close public transport	Record closing of public transport	Ordinal scale	0 - no measures 1 - recommend closing (or significantly reduce volume/route/means of transport available) 2 - require closing (or prohibit most citizens from using it) Blank - no data
C6	C6_Stay at home requirements	Record orders to "shelter-in-place" and otherwise confine to the home	Ordinal scale	0 - no measures 1 - recommend not leaving house 2 - require not leaving house with exceptions for daily exercise, grocery shopping, and 'essential' trips 3 - require not leaving house with minimal exceptions (eg allowed to leave once a week, or only one person can leave at a time, etc) Blank - no data
C7	C7_Restrictions on internal movement	Record restrictions on internal movement between cities/regions	Ordinal scale	0 - no measures 1 - recommend not to travel between regions/cities 2 - internal movement restrictions in place Blank - no data
$C8$	$C8$_International travel controls	Record restrictions on international travel *Note: this records policy for foreign travellers, not citizens*	Ordinal scale	0 - no restrictions 1 - screening arrivals 2 - quarantine arrivals from some or all regions 3 - ban arrivals from some regions 4 - ban on all regions or total border closure Blank - no data
$H1$	$H1$_Public information campaigns	Record presence of public info campaigns	Ordinal scale	0 - no Covid-19 public information campaign 1 - public officials urging caution about Covid-19 2- coordinated public information campaign (eg across traditional and social media) Blank - no data
$C1$, $C2$, $C3$,$C4$, $C5$,$C6$, $C7$ & $H1$	$C1$_Flag, $C2$_Flag $C3$_Flag, $C4$_Flag $C6$_Flag, $C7$_Flag & $H1$_Flag		Binary flag for geographic scope	0 - targeted 1- general Blank - no data

Table 2.2: Containment, closure and Health system polices codebook for the Oxford Covid-19 Government Response Tracker [45]

2.1.4 Google Mobility Trends

We utilise the Google COVID-19 Community Mobility Reports, or Google Mobility data, as the dependent variable in our regression formulation of $\bar{r}_i$. Using mobility data provided by Google, we were able to see how mobility changed for each census division in Ontario [4]. As communities around the globe responded to the COVID-19 pandemic, public health officials suggested that the same type of aggregated, anonymized insights used in applications such as Google Maps could be useful as they make decisions to combat COVID-19 [4]. With this, Google released Community Mobility Reports with the aim to provide researchers and government officials with insight into what changed in response to these COVID-19 containment policies. Google Mobility reports capture total visits to each of the following locations (most commonly visited by individuals and referred to as social mobility indicators):

1. Grocery and pharmacy stores, including grocery markets, food warehouses, farmers markets, specialty food shops, drug stores and pharmacies

2. Parks, consisting of local and national parks, public beaches, marinas, dog parks, plazas and public gardens

3. Transit stations, including subway, bus and train stations

4. Retail stores and recreation outlets such as restaurants, cafes, shopping centers, theme parks, libraries, museums and movie theaters

5. Workplaces

Google creates these aggregated and anonymized data sets from users who have turned on and agreed to share the information from their location history setting of their Google accounts on their phones [4]. As such, these data sets may not be representative of the population, especially in more rural settings with bad data reception or regions where cellphone

usage is lower. Additionally, Google has not publicly shared the precise methodologies for calculating these social mobility scores, thus there is a certain degree of ambiguity as to how representative this data is of true population trends. We discuss this limitation more extensively in Chapter 5. However, through data provided by Statistics Canada, the number of individuals with personal cell phones in Canada as of 2020 was above 80% [11]. Additionally, through data provided by Statista, Google Maps is the most downloaded mapping app in the United States, hence it is the most indicative mobility application for Canadian usage [16].

The daily values of each Google Mobility index are aggregated across individuals in a region who meet the requirement for data sharing. These daily values are calculated relative to a baseline. This baseline is determined to be the median for the corresponding day of the week during the five week period of January 3 to February 6, 2020, thus each daily value is a percent change of the social mobility category relative to its baseline [4].

Within the Google COVID-19 Community Mobility report for Ontario, there are notable trends that can be seen within the data that most likely occur due to factors outside of the forces of COVID-19. For example, we see a periodic trend in the data over the course of 7 day cycle. When one considers this, it is logical that on weekends, certain categories would be lower than weekdays. Most full time workers are not required to come into work on weekends and thus, they will most likely fall within one of the other mobility categories. There is a significant correlation between transit mobility and workplace movements. This is justified as in 2016, it was reported that 92.5% of workers commuted to their place of work by either a personal car or public transit [35].

As we are looking to achieve a broad overview of perceived risk of infection, we chose to look specifically at changes in workplace mobility. Workplaces follow a periodic pattern as every weekend, you have a small portion of the workforce going to their place of work. Retail and recreation are a more sporadic and depend more so upon weather, time of year,

as well as market and personal sentiment.

A caveat to this data is that Google social mobility indicators are available at census division levels within the province of Ontario, however they are unavailable at the broader PHU level. Our later analysis will require the data to be a state we can use in our regression analysis and therefore some data manipulation was required. Google split the mobility data into 51 regions corresponding to local municipalities. PHUs in Southern Ontario follow the boarders of these municipalities for the most part, however there are a few regions that combine to form a single unit. To account for these combined public health regions, we took the average value of percent change among all of the contributing census divisions. In Northern Ontario we faced a challenge as the borderlines of each region do not neatly fit within the bounds of the Northern PHUs . The three most northern PHUs are Northwestern (NWR), Thunder Bay (THB) and Porcupine (PQP) with population densities of $0.4/km^2$, $0.7/km^2$, $0.3/km^2$ respectively. Across these PHUs resides one whole district (either Rainy river, Thunder Bay or Cochrane) plus approximately a third of the landmass of Kenora district (i.e. NWR = Rainy River + $\frac{1}{3}$ Kenora District, THB = Thunder Bay + $\frac{1}{3}$ Kenora District and PQP = Cochrane + $\frac{1}{3}$ Kenora District). We cannot split the Google Mobility data for Kenora amongst each PHU so we must assign it to one. When we look at the Population of Kenora District, the largest communities fall within the Northwestern PHU. These communities account for more than half of the districts population. Thus, for our purposes we will combine the Google Mobility data for Rainy River and Kenora District to form a single set. Table 2.3 outlines the exact census division that fall within each given Public Health Unit:

Public Health Region	Code	Google Mobility Regions
Algoma Public Health	ALG	Algoma District
Brant County Health Unit	BRN	Brant County + Brantford
Chatham-Kent Health Unit	CHK	Chatham-Kent
Durham Region Health Department	DUR	Regional Municipality of Durham
Eastern Ontario Health Unit	EOH	Prescott and Russel + Stormont, Dundas and Glengarry
Grey Bruce Health Unit	GBC	Grey County + Bruce County
Halton Region Health Department	HAL	Regional Municipality of Halton
Hamilton Public Health Services	HAM	Hamilton
Haldimand- Norfolk Health Unit	HDN	Haldimand County + Norfolk County
Haliburton, Kawartha, Pine Ridge District Health Unit	HKP	Haliburton County + Kawartha Lakes + Northumberland County
Hastings and Prince Edward Counties Health Unit	HPE	Hastings County + Prince Edward County
Huron Perth District Health Unit	HPH	Huron County + Perth County
Kingston, Frontenac and Lennox and Addington Public Health	KFL	Frontenac County + Lennox and Addington County
Lambton Public Health	LAM	Lambton County
Leeds, Grenville and Lanark District Health Unit	LGL	Lanark County + Leeds and Grenville United Counties
Middlesex-London Health Unit	MID	Middlesex County
Niagara Region Public Health Department	NIA	Regional Municipality of Niagara
North Bay Parry Sound District Health Unit	NPS	Nipissing District + Parry Sound District
Northwestern Health Unit	NWR	Rainy River District + Kenora District
Ottawa Public Health	OTT	Ottawa
Southwestern Public Health	OXF	Oxford County + Elgin County
Peel Public Health	PEL	Regional Municipality of Peel
Porcupine Health Unit	PQP	Cochrane District
Peterborough Public Health	PTC	Peterborough County
Renfrew County and District Health Unit	REN	Renfrew County
Simcoe Muskoka District Health Unit	SMD	Simcoe County + Muskoka District Municipality
Sudbury and District Health Unit	SUD	Sudbury District
Thunder Bay District Health Unit	THB	Thunder Bay District
Toronto Public Health	TOR	Toronto
Timiskaming Health Unit	TSK	Timiskaming District
Region of Waterloo Public Health	WAT	Waterloo Regional Municipality
Wellington-Dufferin-Guelph Public Health	WDG	Wellington + Dufferin
Windsor-Essex County Health Unit	WEC	Essex County
York Region Public Health Services	YRK	Regional Municipality of York

Table 2.3: PHU regions and their corresponding Google Mobility Regions

2.1.5 Mask Compliance

Using the data provided by the Institute for Health Metrics and Evaluation (IHME), we are able to see the provincial level for Ontario [22]. Through collaborative work done by the Delphi Group at Carnegie Mellon University and University of Maryland "COVID-19 Trends and Impact Surveys", in partnership with Facebook [47], researchers we are able to obtain mask compliance data down to the provincial scale for Canada. Since April 6, 2020, the US COVID-19 Trends and Impact Survey (CTIS) has actively been providing researchers with direct surveys from the general population [47]. A random sample of active Facebook users each day were invited to participate in the survey. If users chose to, they would be redirected to the University of Maryland's website to complete the survey. Through these results, CTIS has been able to collect information regarding COVID-19 symptoms, risks, mitigating behaviours, testing, vaccination and other areas of interest [47]. The survey was updated regularly with input from survey methodologists, epidemiologist and public health specialists to address public health questions that were time-dependent which introduced masking behaviours to the study [47]. Following the work done by Wilson *et. al.* [57], we assume that efficacy of a mask is 50% and the values of mask compliance come from the data provided by IHME [22]. While we are unable to see further to a more refined scale in Ontario, having mask compliance on the provincial scale provides important insight to the trends across Ontario. Using this data, we are able to effectively model a players personal discomfort to complying with NPIs enforced across Ontario given the case numbers of their PHU.

2.2 Computation and Analysis of r_i and $\tilde{r_i}$

We begin our analysis of $\bar{r_i}$ and $\tilde{r_i}$ from March 1^{st}, 2020. While we have case data available starting mid February 2020, there is no consistent start date across all the regression variables

for all 34 PHUs . As we are trying to determine the perceived risk of infection $\bar{r}_i$ and personal discomfort $\tilde{r}_i$, we perform two separate regression analysis for each Public Health Unit. Each player makes a decision whether or not to respect the measures in place by looking at widely available and easy to acquire information. This includes daily cases, daily deaths, provincial hospitalizations and a players perceived risk of infection. In our game discussed in Chapter 3, $\bar{r}_i$ is incurred if a player does not respect NPIs. As a player's estimates are based on the epidemiology of their region, this should directly effect the Google Mobility index of the region. Therefore we view the Google mobility index as a function of regional cases, deaths and provincial hospitalizations which gives us

$$G_{mobil} = v_1(cases(t)) + v_2(deaths(t)) + v_3(hospitalizations(t)) + \bar{r}_i \tag{2.2}$$

When we have no cases, deaths or hospitalizations, we get $\bar{r}_i$.

The computation of $\tilde{r}_i$ follows similarly. In our game framework, $\tilde{r}_i$ is incurred if a player does respect NPIs, and perceives this as a personal discomfort. We postulate that daily mask compliance is affected by daily cases and the stringency of measures placed by the government. We do not include daily deaths in this computation as a players perceived discomfort to wearing a mask does not correspond to the daily deaths in a region. This can be thought of empirically as whether an individual wears a mask is a result that has more to do with stringency measures the government has in place, as well as the number of cases within a region. The more cases there are, the higher the chance of infection due to a contact with another individual in your region. The deaths of a region do not have an impact on mask compliance as whether more people die as a result of the disease does not force or encourage a person to wear a mask. These relationships can be seen explicitly when using a Pearson correlation test. A Pearson correlation test is a commonly used statistical test which measures the linear correlation between two data sets. Specifically, the sample

correlation coefficient

$$c = \frac{s_{x;y}}{s_x s_y}$$

it is the ratio between the covariance of two variables and the product of their standard deviations where s_x is the sample standard deviation of $x_1, \ldots, x_n$

$$s_x = \sqrt{\sum_{i=1}^{n} \frac{(x_i - \bar{x})^2}{n-1}}$$

These correlation coefficients c values range from -1 to 1, signifying a perfectly negative linear correlation and perfectly positive linear correlation respectively. When we perform a Pearson correlation test between regional data and the mask compliance data [22], we find that overall, there is a statistically significant p-value on the scale of 10^{16} relating daily cases and mask compliance whereas the correlation with daily deaths has a p-value of approximately 0.05.

In general, we can view the level of mask compliance as a function of daily cases and the stringency index for Ontario. The multi-linear regression analysis gives us a linear combination of factors which equal mask compliance levels

$$M_{compl} = w_1(cases(t)) + w_2(OxCGRT(t)) + \tilde{r}_i \tag{2.3}$$

When we have no cases or stringency measures enforced, we would get $\tilde{r}_i$. Both computations for $\bar{r}_i$ and $\tilde{r}_i$ capture very broad cases which are sufficient for our research, however possibilities for further refinement are discussed in Chapter 5. Regression analysis was computed using the statistical software R's *lm* function which is used for fitting linear models. To compute the regression problems in R over our values, we fit the original equations 2.2

and 2.3 into the following matrix format

$$\begin{bmatrix} | \\ G_{mobil}(t) \\ | \end{bmatrix} = \begin{bmatrix} | & | & | \\ cases_i(t) & deaths_i(t) & Hosp(t) \\ | & | & | \end{bmatrix}$$

For each one month time increment we run the regression of our input vectors against our output, extract the intercept and store it in a vector. We repeat for each public health unit, collecting the perceived risk of infection and personal discomfort terms into the $\bar{r}_i$ matrix and $\tilde{r}_i$ matrix respectively.

$$\bar{r}_{matrix} = \begin{bmatrix} \bar{r_1}(1) & \bar{r_1}(2) & \dots & \bar{r_1}(10) \\ \bar{r_2}(1) & \bar{r_2}(2) & \dots & \bar{r_2}(10) \\ | & | & \ddots & | \\ \bar{r_{33}}(1) & \bar{r_{33}}(2) & \dots & \bar{r_{33}}(10) \\ \bar{r_{34}}(1) & \bar{r_{34}}(2) & \dots & \bar{r_{34}}(10) \end{bmatrix}$$

Where $\bar{r}_i(t)$ for $i \in \{1, 2, \dots, 34\}$ represents the corresponding PHU via column and $t \in \{1, 2, \dots, 10\}$ is the time increment we are working at, and $\bar{r}_{matrix}$ is the 34×10 matrix. We have a similar matrix for $\tilde{r}_{matrix}$ as seen below.

$$\tilde{r}_{matrix} = \begin{bmatrix} \tilde{r_1}(1) & \tilde{r_1}(2) & \dots & \tilde{r_1}(10) \\ \tilde{r_2}(1) & \tilde{r_2}(2) & \dots & \tilde{r_2}(10) \\ | & | & \ddots & | \\ \tilde{r_{33}}(1) & \tilde{r_{33}}(2) & \dots & \tilde{r_{33}}(10) \\ \tilde{r_{34}}(1) & \tilde{r_{34}}(2) & \dots & \tilde{r_{34}}(10) \end{bmatrix}$$

For our game theoretic approach in Chapter 3, we require the ratio of the personal discomfort of wearing a mask over the perceived risk of infection for every PHU across all

10 months. To do so, we simply take the ratios:

$$r_{ij} := \frac{\bar{r}_{ij}}{\tilde{r}_{ij}}, \qquad i = \{1, \cdots, 34\}, \quad j \in \{1, \cdots, 10\}.$$

2.3 Analysing r_i and $\tilde{r_i}$

With the results determined above, we obtain two matrices for $\bar{r}_i$ and $\tilde{r}_i$. With these matrices, we explored what relationships exist between these determined risk and discomfort factors to gain further insight to what possible variables have an effect on these perceptions. The variables which we used for these correlation tests are median age, median income, average temperature of the PHU and the proportion of population with post-secondary education [7]. In performing these analyses by each month, we found that there are some variables that appear to have a strong correlation at certain times in the year, whereas other showed less correlation at any time. These results are highlighted in Figure 2.1 and the sections below.

2.3.1 Correlation Analysis with Median Age

When we perform the correlation analysis with the **median age** of the population we found most often there is no significant relationship between median age and $\tilde{r}$. Thus, there is lack of evidence of a relationship between an individual's perceived discomfort with mask compliance across all months in question. We did however find that there is an evident relationship between $\bar{r}$ and median age. Specifically we saw the following relationship as outlined in Table 2.4

We can see in this Table 2.4 that for most months there is a linear relationship between the $\bar{r}$ and PHU median age. The most significant relationship we see is in July in which there is a positive correlation, which means as median age increased, the higher an individuals perceived discomfort of NPI would be.

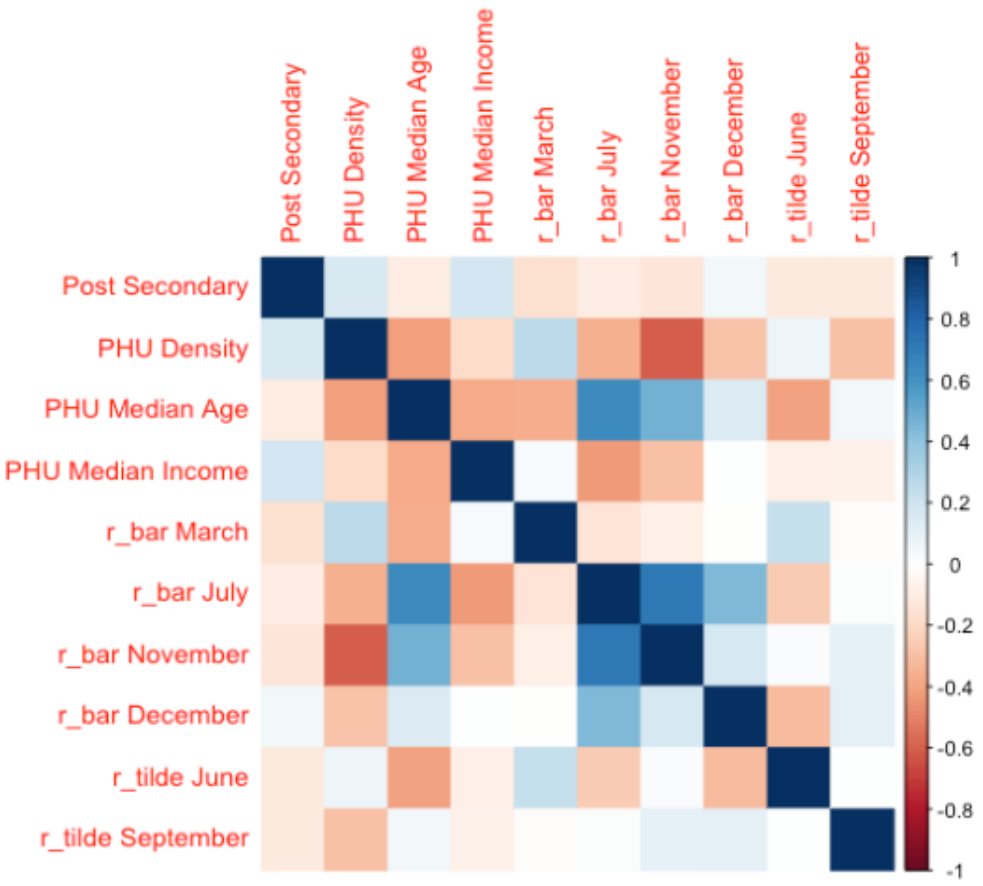

Figure 2.1: Correlation matrix for parameters of interest and significant monthly $\bar{r}$ and $\tilde{r}$ values.

2.3.2 Correlation Analysis With Average Temperature

To determine the average temperature across a given Public Health Unit, we had to take multiple weather radar sources in a given unit and take the average across the monthly recorded temperatures. For smaller regions such as Toronto Public Health Unit, this was a simple task as temperature does not greatly vary within the region. However, for larger units such as Northwestern Health Unit, the temperatures varied across the region. We note that despite these varying temperatures, in these regions the population density is very low (most often under or around one individual per kilometer squared) and most major towns and cities reside further South rather than North. Therefore we assert that these average

Month of 2020	P-value	Correlation Coefficient
March	0.03160	-0.3693
April	0.03978	0.3542
May	0.04337	0.3485307
June	0.01703	0.406551
July	5.545×10^{-5}	0.6346767
August	0.3086	*insignificant*
September	0.1251	*insignificant*
October	0.01123	0.4296008
November	0.004315	0.4772626
December	0.3969	*insignificant*

Table 2.4: Outlines the determined significance of each correlation value of $\bar{r}$ and median age across the 34 PHUs

temperatures are appropriate given the other aspects of these wide-covering PHUs .

When we perform the correlation analyses, we find that most often, there is not enough evidence to suggest a statistically significant relationship. The months with average temperatures and correlations are as follows:

1. For the month of June 2020 and $\tilde{r}$, the correlation estimate is -0.3896 with a p-value of 0.02277, thus signifying that there is a negative linear relationship between average temperature and perceived discomfort of NPIs.

2. In the month of September, we found a correlation value of 0.4489 with corresponding p-value of 0.00774 between average temperature and $\tilde{r}$.

While these estimates encapsulate this relationship between $\tilde{r}$ and average temperature, it is interesting to note that these months, June and September, are times of the year where the school year ends and begins. Despite schools being online for the months prior to and including June, as students began to finish online school, they were more likely to be outdoors, not using NPIs after months inside the house. Contrarily, in September 2020, Ontario tried to let students go back to school with the requirement of NPIs being strictly

used and/or followed.

2.3.3 Correlation Analysis with Post-Secondary Education

Within Ontario's census data, viewers are able to see the proportion of the population, in our case the 34 PHUs , with a post-secondary certificate, diploma or degree [7]. This category includes any individual with an apprenticeship or trades certificate/diploma, certificates of apprenticeship/qualification, College, CEGEP or non-university certificate/diploma and university certificate or diploma above or below a bachelors degree. Across each month and PHU there is no correlation between post-secondary education and perceived risk of infection or personal discomfort with NPI compliance. One possible reason for this could be because we include too many certifications in the post-secondary education category.

2.3.4 Correlation Analysis with Median Income

Using PHU level data from the 2016 census [7], we can extract the median income of a given unit. While these values are constant throughout the year, when we perform the correlation analyses with time-varying risk values, we find a few cases of significant correlation. For the month of April, we determined a negative correlation with perceived risk of infection and median income. The estimated correlation parameter is -0.4397 with a p-value of 0.009271 which suggests that regions with higher incomes have a lower perceived risk of infection. We see this trend again in the month of June and July where perceived risk of infection and median income had a negative correlation, specifically an estimated coefficients -0.3751 and -0.4233 with p-values 0.02882 and 0.01262 respectively. This could be because these higher income regions host more individuals with desk jobs who were confined to working from home, whereas regions with lower incomes may host more individuals who work essential jobs requiring workers to be on-site, such as grocery stores and pharmacies. In such a case,

Month(s) of 2020	P-value	Correlation Coefficient
March-June	> 0.05	*insigni cant*
July	0.03666	-0.3597056
August-September	> 0.05	*insigni cant*
October	0.03064	-0.3712462
November	0.0001748	-0.6002718
December	0.1063	*insigni cant*

Table 2.5: Correlation analysis between PHU population density and $\bar{r}$

as they are on the front-line working during the pandemic, they do not have the luxury of a avoiding exposure.

2.3.5 Correlation Analysis with Population Density

When performing the correlation analysis with population density, we found that it wasn't until May that there was a statistically significant relationship. In May 2020, we determined there to be a positive correlation of value of 0.5353 and p-value of 0.001107 between population density and personal discomfort with NPI compliance. This suggests that for the month of May, as population density increased, the perceived discomfort with NPI increased, as people in denser areas were perhaps more eager to socialize. After this month however, there were no statistically significant relationships between $\tilde{r}$ and PHU population density.

The perceived risk of infection held a relatively steady relationship with PHU population density across 2020. Our findings are outlined in Table 2.5

We can see that in the first months of the pandemic, there was no statistically significant relationships between population density and perceived risk of infection. When considering the measures that were enforced, most individuals could not go outside their primary residence other than for essential purposes [8]. As of July 2020, we begin to see a negative relationship between population density and perceived risk of infection. Individuals in denser regions had lower perceived risks of infection as NPIs took a larger toll on their lives.

This toll is especially seen in populations living in smaller spaces, such as condos and apartments, multi-generational households and those with children who are forced to stay home due to school closures. This frustration leads to NPI fatigue and diminishes an individuals perception of infection. Hence while these associations are atypical [59], the NPI fatigue experienced by residents of dense regions serves as a reason for the negative correlation seen between population density and perceived risk of infection.

Chapter 3

The NPI Compliance Game

Our model has 34 interacting groups whose decisions affect each other's perceived relative risk of infection. That is to say we have a game taking place between population groups. To set up our game, we review the concept of an n-person game. An n-person game is one in which each player has a finite set of pure strategies and a definite set of payments to the n players which correspond to each n-tuple of pure strategies, one strategy being taken for each player [38]. Mixed strategies are probability distributions over the pure strategies with payoff functions as the expectations of the players. Hence mixed strategies take polylinear forms in the probabilities with which the various players play their pure strategies [38]. A Nash equilibrium is an outcome from a game in which once achieved, no player can increase their payoff by switching strategies [38]. If most of the population adopts strategy P and individuals who adopt another strategy Q always obtain a lower payoff than those adopting P, then P is said to be a Nash equilibrium. If most individuals adopt strategy Q however, individuals adopting a strategy that is closer than Q to P obtain a higher payoff for any $Q \neq P$, then P is said to be convergently stable. If P is a Nash equilibrium and all payers are currently playing P, then noone should change strategy. If P is convergently stable, then regardless of what strategy is most common in the population, individuals should start to

play strategies closer to P and ultimately adopt P. It is generally expected that a strategy observed in a real population must be a convergently stable Nash equilibrium.

A multiplayer Nash game consists of a finite number of players denoted by $N > 0$. A generic player $i \in \{1, \ldots, N\}$ has a strategy vector x_i selected from a closed convex set $S_i \subset \mathsf{R}^{n_i}$ so that $n_1 + \cdots + n_N = n$. A player has a payoff function $u_i : K \longrightarrow \mathsf{R}$, where $K := S_1 \times \cdots \times S_N$ or the cross product of the strategy sets of all players; evidently: $K \subset \mathsf{R}^{n_1 + \cdots + n_N = n}$. In general we strive to find a Nash equilibrium strategy vector $\underline{x} := (x_1, x_2, \ldots, x_N)$, such that when player $i \in \{1, \ldots, N\}$ plays x_i, there is no reason to switch strategies and as such, these strategies should be stable equilibrium solutions of our game. A Nash equilibrium is the most common way to define the solution to a non-cooperative game involving two or more players [44]. Mathematically, we define a Nash vector of strategies as follows:

Definition 1. *Assuming each player is rational and wants to minimize their payo function* $u_i : K \longrightarrow \mathsf{R}$. *Then a* ***Nash equilibrium*** *is a vector* $x \in K$ *which satis es the inequalities:*

$$u_i(x_i, \hat{x}_i) \leq u_i(x_i, \hat{x}_i), \ \forall i \in \{1, \ldots, N\}, \ \forall x_i \in S_i, \ \textit{where}$$

$$\hat{x}_i := (x_1, \ldots, x_{i \ 1}, x_{i+1}, \ldots, x_N)$$

For simplicity's sake, we assume that all players in any given PHU are provided with the same information and use this information to asses their risks and discomforts. We let $N = 34$ and $i \in \{1, \ldots, 34\}$, representing an average player in each of the 34 PHUs in Ontario. Each group represents a fixed proportion of the population ϵ_i where $\epsilon_i \in (0, 1)$ and $\sum_{i=1}^{34} \epsilon_i = 1$. As determined in Chapter 2, each population group differs in their perceived risk of infection $\bar{r}_i$ and personal discomfort with NPIs $\tilde{r}_i$. We recall the previously determined

$r_i \coloneqq \frac{r_5}{r_i}$ which is the relative perceived risk/discomfort of complying with NPIs. The strategy of any player $i \in \{1, \cdots, 34\}$ is the probability that they will comply with NPIs, denoted by $x_i \in [0, 1]$, hence the strategy set for our game will be $K \coloneqq [0, 1] \times \cdots \times [0, 1]$.

While in previous work [14, 20], authors have a different set up for their utility functions, we utilise a different approach. In 2007, Cojocaru *et. al.* worked with childhood diseases such as measles and pertussis ("whooping cough") which have a tremendous amount of data and research available detailing transmission values to guide the determination of epidemiological constraints [20]. Additionally, other researchers used equilibrium solutions of a deterministic Susceptible-Infected-Recovered (SIR) compartmental model with the assumption that individuals have perfect knowledge of their probability of infection [14]. In both models, authors define a function π_p to represent the perceived probability of becoming infected given the proportion p of the population that is vaccinated. We adopt a similar utility function as in [20], unfortunately we do not have the same information for COVID-19 as for these well known diseases, thus we make the following modification to our game.

$$U_i(t) = r_i x_i(t) + \Big(1 - eff_{NPI}(t)\Big) \sum_{i=1}^{34} \epsilon_i x_i(t) \Big(1 - x_i(t)\Big), \text{ for each } t \in \{1, \cdots, 10\} \quad (3.1)$$

This form of the utility function implies that disease prevalence is a function of how many individuals comply with NPIs as well as the perceived efficacy of the enforced NPIs (denoted here by $eff_{NPI} \in [0, 1]$). A greater perceived coverage in the population means a reduced perceived infection risk for susceptible individuals.

3.0.1 Solving n-player Games

In this thesis, we use a projected dynamical systems (PDS) approach to gain greater analytic capabilities, including the ability to visualise the structure of the dynamic game through theoretical analysis as well as compute the optimal strategy and respective equilibrium NPI

compliance coverage.

First, we review the definitions of a few fundamental mathematical concepts on the Euclidean space R^k, for any finite dimension $k > 0$. For K to be closed, the compliment of K, denoted by $\overline{K}$, is an open set, $\forall x \in \overline{K},\ \exists\ \epsilon > 0\ s.t.\ B(x, \epsilon)\ \subseteq \overline{K}$. A subset $K \subset \mathsf{R}^k$ is said to be convex if for any $x, y \in K$ and any $\lambda \in [0, 1]$, the point $\lambda x + (1 - \lambda)y$ is an element of the space K. The mapping $F : K \longrightarrow \mathsf{R}^k$ is convex if $\forall x, y \in K, \lambda \in [0, 1]$, we have

$$F\Big(\lambda x + (1 - \lambda)y\Big)\ \leq\ \lambda F(x) + \big(1 - \lambda\big)F(y)$$

In our work, we will require a projection operator whose definition requires an understanding of normal cones and tangent cones.

Definition 2. *Let $K \subset \mathsf{R}^k$ be a non-empty, closed, convex subset with $\bar{x} \in K$. The set of all vectors that are tangent to K at a point $\bar{x} \in K$ is called the **tangent cone** to K at $\bar{x}$ and is denoted by*

$$T_K x \coloneqq \overline{\bigcup_{h>0} \frac{K - x}{h}}$$

Definition 3. *Let $K \subset \mathsf{R}^k$ be a convex set with $\bar{x} \in K$. The **normal cone** to K at $\bar{x}$ is*

$$N(\bar{x}; K) \coloneqq \{x\ \ \in \mathsf{R}^k | \langle x\ , x - y\rangle \leq 0,\ \forall y \in K\}$$

We let $N(\bar{x}; K) \coloneqq \emptyset,\ \forall \bar{x} \notin K$

Using definitions 2 and 3 we define **projection operator** of R^k onto K as an operator $P_K : \mathsf{R}^k \to K$ which satisfies

$$\|P_k(z) - z\| = \inf_{x2K} \|x - z\|$$

In other words, when the operator P_K acts on a vector $z \in \mathsf{R}^k$, the result is a vector

$P_K(z) \in \mathsf{R}^k$ which determines the minimum distance between the vector z and the set K. The many properties of projection operators are discussed in length by author Eduardo Zarantonello [62] however, authors note that a projection is not always differentiable outside of it's range. We can however estimate its one-sided directional derivative $\Pi_K(x, v)$ where $x \in K$ and $v \in \mathsf{R}^k$ is any directional vector. The vector projection operator $\Pi_K(x, v) = P_{T_K(x)}(v)$ which projects v onto the tangent cone to K at x is defined as

$$\Pi_K(x, v) \coloneqq \lim_{! \; 0^+} \frac{P_K(x + \delta v) - x}{\delta} \;\Rightarrow\; \Pi_K(x, v) = P_{T_{K(x)}}(v)$$

Note that Π_K is discontinuous on the boundary of the set K. The characteristic of this operator we use is a consequence of Moreau's Theorem which states that $\exists n \in N_K(x),\ s.tv = \Pi_K(x, v) + n$. For a proof of this theorem, refer to [18]. Using this, we obtain the following result which gives us the existence of the PDS.

theoremet $K \subset \mathsf{R}^k$ be a non-empty, closed, convex subset. Suppose $x_0 \in K$ and assume $F : K \to \mathsf{R}^k$ is a Lipschitz continuous vector field. Then, the initial value problem

$$\frac{dx(\tau)}{d\tau} = \Pi_K\Big(x(\tau),\ -F(x(\tau))\Big),\quad x(0) = x_0 \in K \tag{3.2}$$

has a unique absolutely continuous solution on the interval $[0, \infty)$

We finally arrive at the formal definition for a projected dynamical system which is given by the solutions to Equation 3.2.

We now show the connection between a Nash game and a PDS.

theorempdsnash Provided the utility functions u_i are of class C^1 and concave (u_i is convex) with respect to the variables x_i, then $x\ \in K$ is a Nash equilibrium if and only if it satisfies the problem:

$$\Big\langle F(x\ ), x - x\ \Big\rangle \geq 0,\ \forall x \in K$$

where $F(x) = (\bigtriangledown_{x_i} u_1(x), \ldots, \bigtriangledown_{x_m} u_m(x)) = \left(\frac{\partial u_i(x)}{\partial x_{i1}}, \ldots, \frac{\partial u_i(x)}{\partial x_{in}}\right)$, which is to say if and only if

$$\frac{dx(\tau)}{d\tau} = \Pi_K\Big(x(\tau), -F(x(\tau))\Big), \;\; x(0) = x_0 \in K \tag{3.3}$$

In our case

$$\bigtriangledown_i U_i = -\frac{\partial U_i}{\partial x_i} = -r_i - (1 - eff_{NPI}) \sum_{i=1}^{34} \epsilon_i\Big(1 - 2x_i(t)\Big) \tag{3.4}$$

To show that our game has a unique solution, we must first recall the following definitions

Definition 4. *Let x be a critical point of the projected Equation 3.2. Then x is a **local strict monotone attractor** if there exists a neighborhood $N(x\ ) \subset K$ of x , so that for any trajectory $x(\tau)$ of Equation 3.2 starting at $x_0 \in N(x\ )$, the function $\tau \mapsto \|x(\tau) - x\ \|$ is decreasing*

We call x a **global strict monotone attractor** if Definition 4 is satisfied for trajectories of Equation 3.2, starting at any point $x_0 \in K$. With these definitions, we present the following theorem from [20]

theorem monotonicity$_u nique_s ol The Nash game introduced earlier has a unique solution. This solution is a gl$

Following the proof of this theorem in [20], we show that our Nash game has a unique solution.

Proof. We begin by showing that the field $F : K \to \mathsf{R}^k$ is strictly monotone on K. We can show this by recalling that for differentiable functions like F, strict monotonicity is equivalent to the following (see [37])

$$\underline{P}^T(\bigtriangledown F)\underline{P} > 0, \quad \text{for all } \underline{P} \neq 0 \in \mathsf{K} \tag{3.5}$$

In our case we have the following,

$$\bigtriangledown F = - \bigtriangledown U_i = 2(1 - eff_{NPI})$$

Using Equation 3.5, we have that

$$\underline{P}^T(\bigtriangledown F)\underline{P} = \underline{P}^T\Big(2(1 - eff_{NPI}\Big)\underline{P}$$

Since $P_i \in [0, 1_p]$ with $1_p < 1$

$$\Rightarrow \underline{P}^T(\bigtriangledown F)\underline{P} > 0$$

Next, we show that $-F : K \to \mathsf{R}^k$ is a vector field with linear growth, meaning there exisits an $M > 0$ such that

$$\| - F(\underline{P})\| \leq M(1 + \|P\|), \quad \forall P \in \mathsf{K}$$

We have that

$$\begin{aligned}
\| - F(\underline{P}\| &= \left[\Big(- r_i - (1 - eff_{NPI}) \sum_{i=1}^{34} \epsilon_i(1 - 2x_i(t))\Big)^2 P\right]^{1=2} \\
&\leq \left(\|\underline{r}_i\| + \left\|(1 - eff_{NPI} \sum_{i=1}^{34} \epsilon_i(1 - 2x_i(t))\right\|\right)\|P\| \\
&\leq M(1 + \|P\|)
\end{aligned}$$

Where $M = \|r\| + \left\|\Big(1 - eff_{NPI} \sum_{i=1}^{34} \epsilon_i(1 - 2x_i(t))\Big)\right\|$

□

3.0.2 34-player Game and NPI compliance

When we solve the game, we solve for the Nash solution x_i for each PHU in Ontario. Each x_i represents a given player in region i's probability of respecting NPIs. We assume here that eff_{NPI} is an average of 50% overall in Ontario. This is an assumption needed to solve the game, we will further address it in the next Chapter. Using the general optimization solver SOLNP from MATLAB and the PDS formulation of the game as in Theorem **??**:

$$\min \quad U_i(x) = r_i x_i(t) + \Big(1 - eff_{NPI}(t)\Big) \sum_{i=1}^{34} \epsilon_i x_i(t) \Big(1 - x_i(t)\Big)$$

$$s.t. \quad x_i(t) \in [0, 1]$$

for each $i \in \{1, 2, \ldots, 34\}$ and for each fixed $t \in \{1, \cdots, 10\}$. This gives us x_i for each region. With these regional probabilities, we are able to determine the expected NPI-compliance level for Ontario, namely: $NPI_{compl} := \sum_{i=1}^{34} \big(\epsilon_i x_i(t)\big)$. We present the determined NPI_{comp} for each month in Figure 3.1:

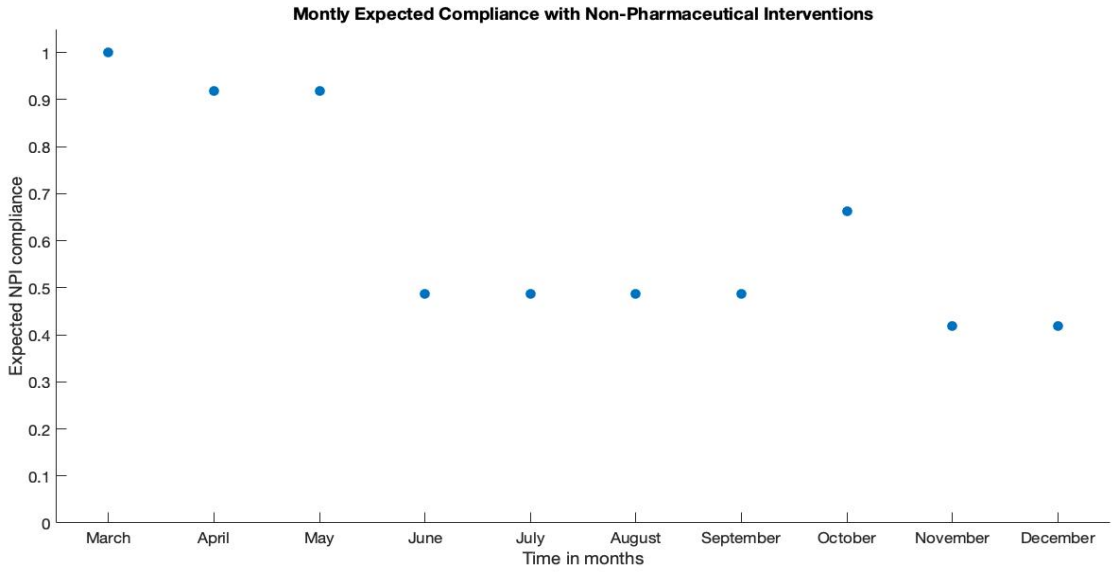

Figure 3.1: Monthly expected NPI compliance across Ontario from March to December 2020

We see expected NPI compliance is initially high and then falls slightly over the months of April and May. In June 2020, there was a large fall in expected NPI compliance which continued over the summer months. The lack of NPI compliance over these months can be attributed to a number of reasons. Specifically, with these warmer months, we saw residents disregarding emergency state orders imposed by the provincial and federal government [8]. In October we see expected NPI compliance rise again which can be attributed to the rise in daily cases within Ontario. To end the year, we see the expected NPI compliance fall to an all time low. This can be attributed to COVID-19 fatigue as well as the many individuals who, despite lockdown orders being imposed, met with family and friends over the holidays. In the next section, we look at the Nash equilibria x_i across five density dependent-groups and investigate how these probabilities of respecting NPIs vary over the year.

3.0.3 Regions of Varying Population Densities and Their Probability of Respecting NPIs

Across figures 3.2- 3.5, we see a large dip in the probability of respecting NPIs from June to September of 2020. As this is seen across multiple regions of varying population densities, this can be attributed to the disregard most individuals had for COVID measures over the summer months as cases and death counts fell. In October 2020, we saw daily case and death counts climb up continuously and thus as perceived risks of infection changed, so did the probability of respecting NPIs. This effect is short lived as most regions saw these probabilities fall. A possible explanation is that as COVID-19 fatigue set in, individuals broke stay-at-home orders to visit their family and friends over the holidays. Another common theme amongst these figures is that of consistently high probabilities of respecting measures. Specifically we look at North Bay Parry Sound Health Unit in Figure 3.2, Huron Perth Health Unit 3.3, Simcoe Muskoka District Health Unit 3.4 and the City of Hamilton Public Health

Services 3.5. Across all of these regions, the probability of NPI compliance stays consistently high across the year. This could be attributed to the vast amounts of Provincial parks and secondary homes in these regions. Seasonal travel threatened the northern PHUs as visitors from highly dense regions brought the threat of COVID-19 outbreaks. Consequentially, the Ontario Government urged residents to remain in their primary dwellings as these Northern health units cannot handle the COVID-19 burden they would ultimately bring. Thus a possible explanation to these consistently high probabilities is the desire to better protect these smaller health care systems.

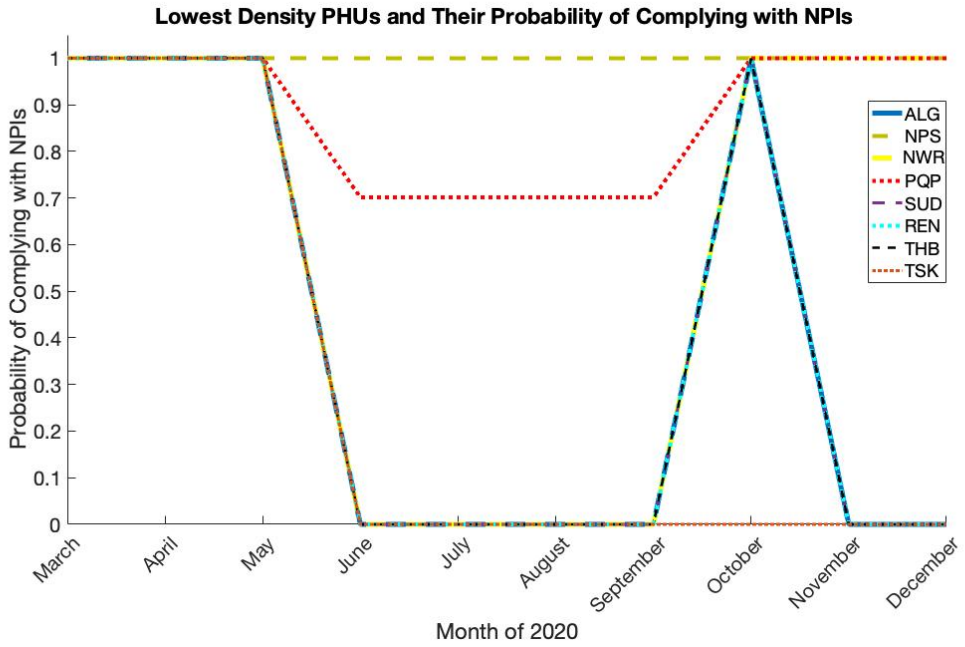

Figure 3.2: Probability of respecting NPIs over 2020 in the PHUs with the lowest population density

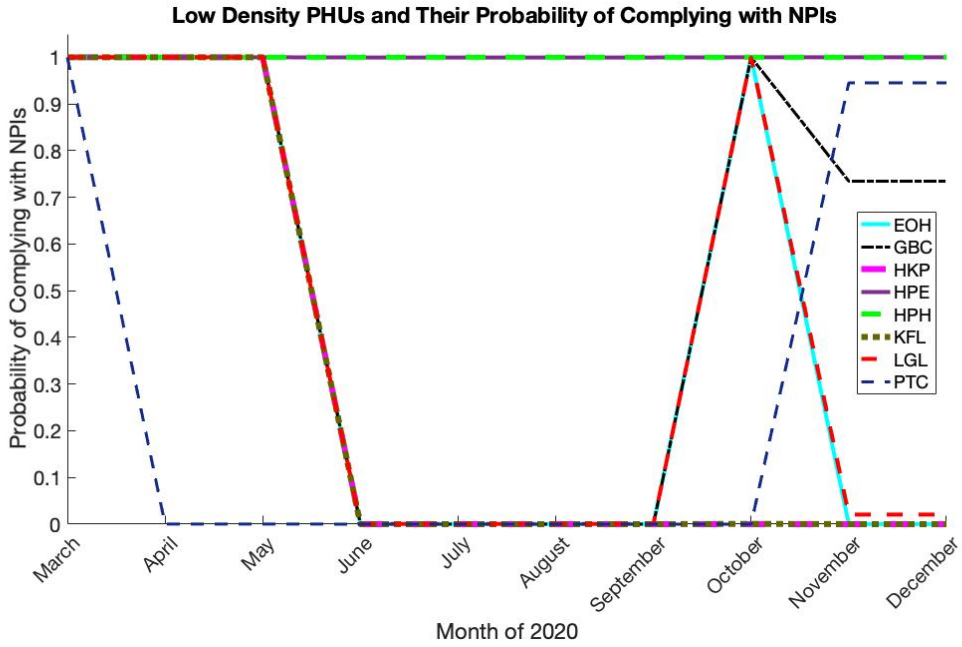

Figure 3.3: Probability of respecting NPIs over 2020 in the PHUs with the second lowest population density

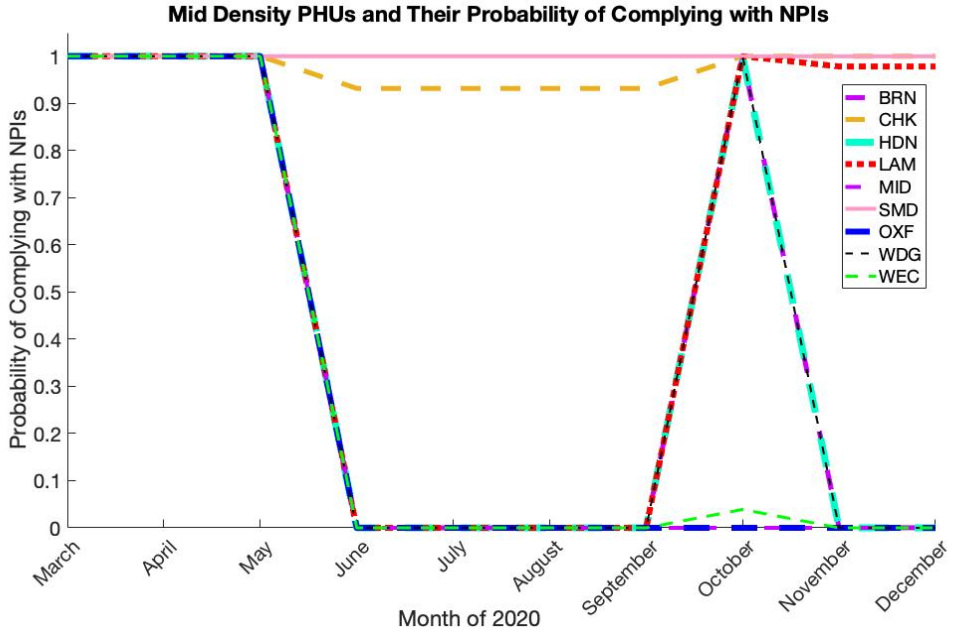

Figure 3.4: Probability of respecting NPIs over 2020 in the PHUs with mid population density

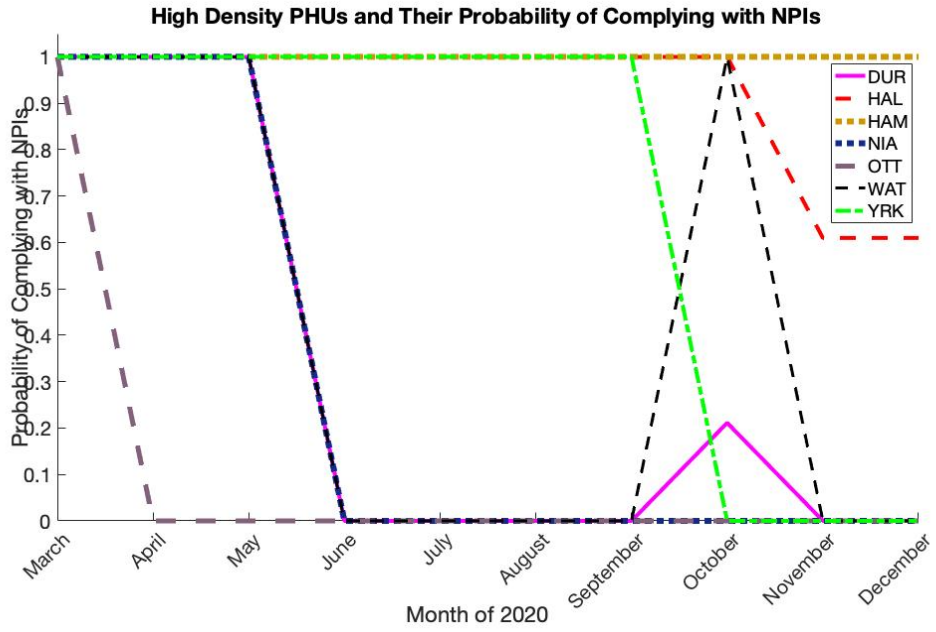

Figure 3.5: Probability of respecting NPIs over 2020 in the PHUs with the second highest population density

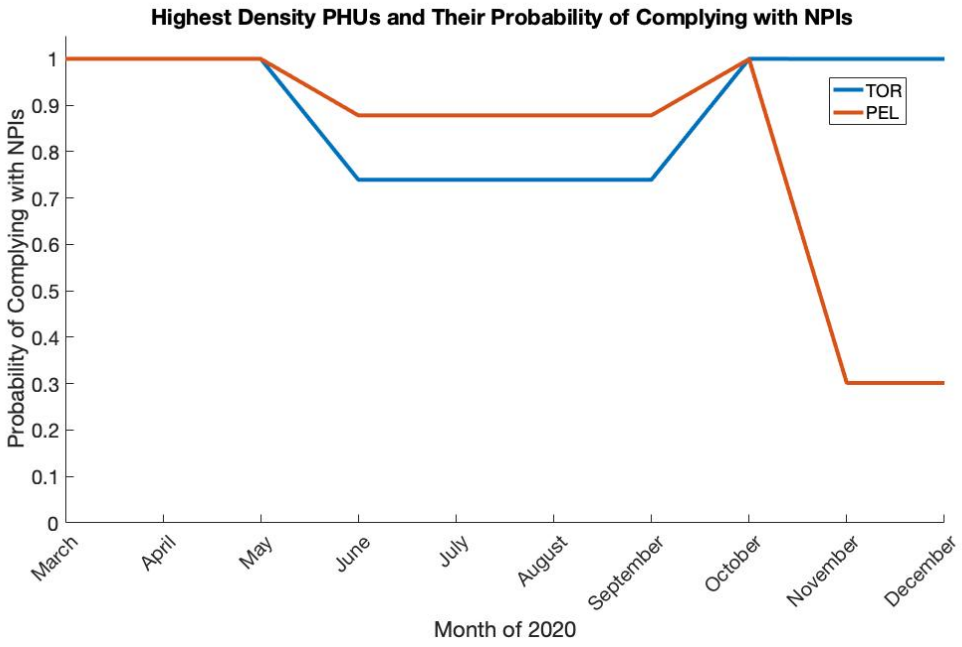

Figure 3.6: Probability of respecting NPIs over 2020 in the PHUs with the highest population density

Despite this strong similarity amongst the different population density groups, we see some differing trends in more densely populated regions. A noticeable quality to Figure 3.3 is the immediate drop in the probability of the Peterborough Public Health. Residents in this region maintain a low compliance rate until October, where we see a steep rise to a high probability of respecting NPIs for the remaining months of 2020. This could be attributed to the lack of cases this Health Unit saw. Specifically, there was not a continual increase in daily cases within this region until end of September 2020. Lambton public health unit had a similar experience to that of Peterborough as seen in Figure 3.4. Grey Bruce Health Unit and Halton Public Health had similar experiences as October brought about a rise in case numbers which the region had not yet seen. After this month, both regions experienced a decrease in the probability of respecting NPIs. Therefore we can attribute the higher probability of NPI compliance in these regions to be a result of the consistently high case numbers the region saw continuously for the first time in 2020. However in the final months of 2020, these probabilities dropped as individuals broke COVID-19 restrictions.

In Figure 3.5, we see that the probability of Ottawa's PHU respecting NPIs dropped after March and remained at zero for the rest of 2020. This is intriguing as Ottawa is the capital of Ontario, with many government officials residing in the city. Despite this and the many cases seen within the region, there was a disregard for non pharmaceutial interventions. This was shown in classic media through news articles and reports provided by CTV News Ottawa, with one such article citing dramatic increase in case numbers around the holidays in 2020 [46]. While York Region Public Health held a strong probability for most of the year until October, this probability subsequently fell to zero. For all remaining regions in the "high population density" group, as June approached, the probability of NPI compliance dipped, in most cases quite low. In October, these probabilities rose to once again fall in November.

The two regions with the highest population densities are Toronto and Peel Figure 3.6. Within these two regions we see a continually high probability of respecting NPIs until June.

While Toronto's probability drops lower than Peel's for the next four months, they both rise to a probability of one. While Toronto maintained a high probability, Peel experienced a large drop, which remained at just above 30% for the remaining months of 2020. Despite the large increase in case numbers Peel experienced in the last months of 2020, we can attribute this low probability of respecting NPIs to be result of COVID-19 fatigue and individuals desires to see family over the holidays.

In the next chapter, we evaluate how good of an estimate our game model is through the use of the expected NPI-compliance determined above.

Chapter 4

Expected Compliance and Real Data Analysis

In this Chapter, we look to investigate the effects of non-pharmaceutical interventions on disease transmission. Moreover, we look to see how accurate our estimates are when using the determined expected NPI compliance rate from the previous chapter.

In epidemiology, R_{eff} is a monitoring indicator to quantify the control of a pandemic as well as the effectiveness of interventions, and in our case, the use of NPIs. Transmission of the virus SARS-COV-2 depends upon the rate of person-to-person contact as well as the probability of transmission given one significant contact between an infected and susceptible individual. Previous work has highlighted that the probability of transmission per contact is reduced through the use of NPIs, specifically with the use of masks ([34, 23]). In conjunction with face mask usage, social distancing measures are a critical tool for slowing pandemic growth. As discussed in Chapter 2, the ways in which we include these social distancing factors in our model are through the use of Google mobility data in Equation 2.2.

4.1 SEIRL Model

Following [34], we use an SEIRL (Susceptible, Exposed, Infectious, Recovered and isoLated) model with daily incidence data across Ontario and at the PHU level. In [34] authors quantify the effectiveness of NPI across Ontario and other countries/regions using the effective reproduction number R_{eff}. Here we show how our expected NPI_{compl} affects R_{eff} for Ontario. Given that we look at several regions across Ontario, another intriguing investigation we conduct is the time varying map of initial infection. We achieve this by determining the size and onset of R_0 for each PHU to provide insight to how the initial wave of transmission spread across the province.

We describe our SEIRL model as follows. Susceptible individuals (S) who are exposed to the virus enter the exposed (E) category for an average of $\frac{1}{}$ days after which they become contagious, moving them into the infected (I) compartment. In general, there is a proportion a of infected individuals who will develop no symptoms (we call this asymptomatic, denoted by I^A) while the remaining $1-a$ compose the infected symptomatic individuals (I^S). Initially, the entire population N_{total} is susceptible. Thus, the expression for our infected compartment is as follows:

$$I(t) = I^A(t) + I^S(t) = \Psi I(t) + (1 - \psi)I(t) \tag{4.1}$$

A proportion $\epsilon > 0$ of $I^S(t)$ will self-isolate into the isolate (L) compartment with a delay of $\frac{1}{}$ days which accounts for test result wait time and/or individuals who may initially disregard minor symptoms [34]. After $\frac{1}{}$ days, individuals either recover from or fall victim to their infection and move into the recovered (R) compartment. With this, we obtain the following

system of equations:

$$\begin{cases} \frac{dS}{dt} & = -\beta S(t)\frac{I}{N_{total}} \\ \frac{dE}{dt} & = \beta S(t)\frac{I(t)}{N_{total}} - \sigma E(t), \\ \frac{dI}{dt} & = \sigma E(t) - \gamma I(t) + \epsilon(\gamma - \kappa)(1-\psi)I(t), \\ \frac{dL}{dt} & = \epsilon\kappa(1-\psi)I(t) - \gamma L(t), \\ \frac{dR}{dt} & = \gamma(1-\epsilon(1-\psi))I(t) + \gamma L(t) \end{cases} \tag{4.2}$$

The model parameters are given in the Table 4.1 with references corresponding to how these values were determined.

Symbol	Definition	Initial Value	Reference
N_{total}	Population size	[7]	-
σ	Rate per day at which exposed individuals become infectious	$\frac{1}{2.5}$	[53]
ψ	Proportion of permanently asymptomatic cases	0.5	[33],[27],[10]
ϵ	Proportion of compliance with isolation	0.95	Assumed
κ	Delay in isolation (days)	1	Assumed
γ	Recovery/removal rate	$\frac{1}{7}$	[60]

Table 4.1: Parameter values for SEIRL model

The disease free equilibrium implies that $S(0) = N$, as mentioned above, and I(0) = 0. Near this disease-free equilibrium, the Jacobian matrix for the system of equations 4.2 is:

$$J = \begin{pmatrix} 0 & 0 & -\beta & 0 & 0 \\ 0 & -\sigma & \beta & 0 & 0 \\ 0 & \sigma & -\gamma + \epsilon(\gamma - \kappa)(1-\psi) & 0 & 0 \\ 0 & 0 & \epsilon\kappa(1-\psi) & -\gamma & 0 \\ 0 & 0 & \gamma(1-\epsilon(1-\psi)) & \gamma & 0 \end{pmatrix}$$

(4.3)

4.2 Ontario's Effective Reproduction Numbers by Public Health Unit

Following the work done by in [54], we use the next generation method to determine our R_0. The next generation method was originally proposed in 1990 by Diekmann, Heesterbeek, and Metz [28] and elaborated upon by van den Driessche and Watmough [55], giving a way to determine R_0 for a compartmental ODE model. Below we give a brief description and outline of the method; proofs and further details can be found at [28, 55].

Let $x = (x_1, x_2 \ldots, x_n)^T$ be the number of individuals in each compartment where the first $m < n$ compartments contain infected individuals. We assume the DFE x_0 exists and is stable and the linear equations for infected $x_1, \ldots x_m$ at x_0 are decoupled. Consider equations written in the form

$$\frac{dx_i}{dt} = F_i(x) - V_i(x)$$

for $i = 1, 2, \ldots, m$. We split equations this way, $F_i(x)$ is the rate of appearance of new infections in compartment i and $V_i(x)$ is the rate of other transmissions between compartment i and other infected compartments. We define $F = \frac{@F_i(x_0)}{@x_j}$ and $V = \frac{@V_i(x_0)}{@x_j}$ for $1 \leq i, j \leq m$, and assume that $F_i, V_i \in C^2$ and $F_i = 0$ if $i \in [m+1, n]$ [54]. From the biological context of F and V, it follows that F is entrywise non-negative and V is non-singular, which gives an entrywise non-negative V^{-1}. Then entry (i, j) of matrix FV^{-1} is equal to the expected number of secondary infections in compartment i, produced by an infected individual in compartment j. We define FV^{-1} to be the **next generation matrix** which gives us $R_0 = \rho(FV^{-1})$ where ρ denotes the spectral radius [54].

In [54] the authors determine R_0 to be the largest eigenvalue of the next-generation matrix. For our model we therefore find thee following closed form expression for R_0:

$$R_0 = \frac{\beta}{(\epsilon\gamma\psi - \epsilon\kappa\psi - \epsilon\gamma + \epsilon\kappa + \gamma)} \tag{4.4}$$

Further, following [32], we compute the eigenvalues of the reduced Jacobian and determine there is one positive eigenvalue which we denote by ρ responsible for growth near the DFE. It can be derived in closed-form as:

$$\rho := \frac{-\epsilon\gamma a + \epsilon\kappa a + \epsilon\gamma - \epsilon\kappa - \gamma - \sigma}{2} + \sqrt{\frac{\epsilon^2\gamma^2a^2 - 2\epsilon^2\gamma\kappa a^2 + \epsilon^2\kappa^2a^2 - 2\epsilon^2\gamma^2a + 4\epsilon^2\gamma\kappa a - 2\epsilon^2\kappa^2a + \epsilon^2\gamma^2 - 2\epsilon^2\gamma\kappa + \epsilon^2\kappa^2}{4}} + \sqrt{\frac{2\epsilon\gamma^2a - 2\epsilon\gamma\kappa a - 2\epsilon\gamma a\sigma + 2\epsilon\kappa a\sigma - 2\epsilon\gamma^2 + 2\epsilon\gamma\kappa + 2\epsilon\gamma\sigma - 2\epsilon\kappa\sigma + 4\beta\sigma + \gamma^2 - 2\gamma\sigma + \sigma^2}{4}}$$

which is solved to determine an expression for β as a function of the growth factor ρ near the DFE:

$$\beta = \beta(\rho) := \frac{\epsilon\gamma a\rho + \epsilon\gamma a\sigma - \epsilon\kappa a\rho - \epsilon\kappa a\sigma - \epsilon\gamma\rho - \epsilon\gamma\sigma + \epsilon\kappa\rho + \epsilon\kappa\sigma + \gamma\rho + \gamma\sigma + \rho^2 + \rho\sigma}{\sigma}. \tag{4.5}$$

Finally, we can rewrite basic reproduction number R_0 as a function of the growth factor ρ near the DFE for each region:

$$R_0(\rho) = \frac{\epsilon\gamma a\rho + \epsilon\gamma a\sigma - \epsilon\kappa a\rho - \epsilon\kappa a\sigma - \epsilon\gamma\rho - \epsilon\gamma\sigma + \epsilon\kappa\rho + \epsilon\kappa\sigma + \gamma\rho + \gamma\sigma + \rho^2 + \rho\sigma}{\sigma((\epsilon\gamma a - \epsilon\kappa a - \epsilon\gamma + \epsilon\kappa + \gamma))} \tag{4.6}$$

To estimate ρ, the exponential growth factor of each region, authors in [29] used the respective weekly case incidence data ($inc(t)$) with the assumption that incidence data is given by an

exponential curve, meaning $inc(t) = inc(0)e^{(t)}$. With this, we can isolate for $\rho(t)$:

$$\rho(t) = \ln \frac{inc(t+1)}{inc(t)}, inc(t) \neq 0 \tag{4.7}$$

Further, in [29] authors identify the fastest phase of nearly unchecked growth, meaning no interventions or mandates, in a given region using a piecewise linear fit to the log of the incidence as in Equation 4.7. This is determined using the R function dpseg() [23, 29]. This function uses a dynamic programming algorithm to generate an optimal piecewise linear fit to a time series, which scores the goodness of the fit between data points with a penalty based upon the number of segments added. Taking the earliest segment with the steepest slope gives us the corresponding initial near-unchecked exponential growth value ρ.

Using all the above results we compute here the ρ_i value for each PHU in Ontario which gives us $R_0^i, i \in \{1, 2, \ldots, 34\}$ using equation (4.6). To determine the 34 ρ values across the Ontario PHUs using 4.7 and dpseg, we require the difference of case numbers between two consecutive weeks in a given PHU to be greater than 0. While some regions had cases as of the first week of March 2020, other regions did not see case numbers appear or increase until late March, early April. Thus, while the start dates for ρ are not the same, the determination for each region follows the same procedure with appropriate start dates depending upon their region. We were able to obtain all 34 R_{0i} values which can be seen in Figure 4.1

Using Figure 4.1, we can see not only the magnitude of these R_0 values but the weeks in which they occur. Taking this more granular view allows us to see how the disease spread amongst the public health units. We see that the regions where R_0 are first determined are those with higher population densities, Halton (568.9 $/km^2$), Peel (1108.1 $/km^2$), Toronto (4334.4 $/km^2$), Waterloo (390.9 $/km^2$) and York (629.9 $/km^2$). With R_0 values ranging from 1.6 to 1.9, disease began to spread to neighboring regions, however it was not until week 3 that these R_0 values began to increase in 13 new regions. By week 4 another 10 regions saw

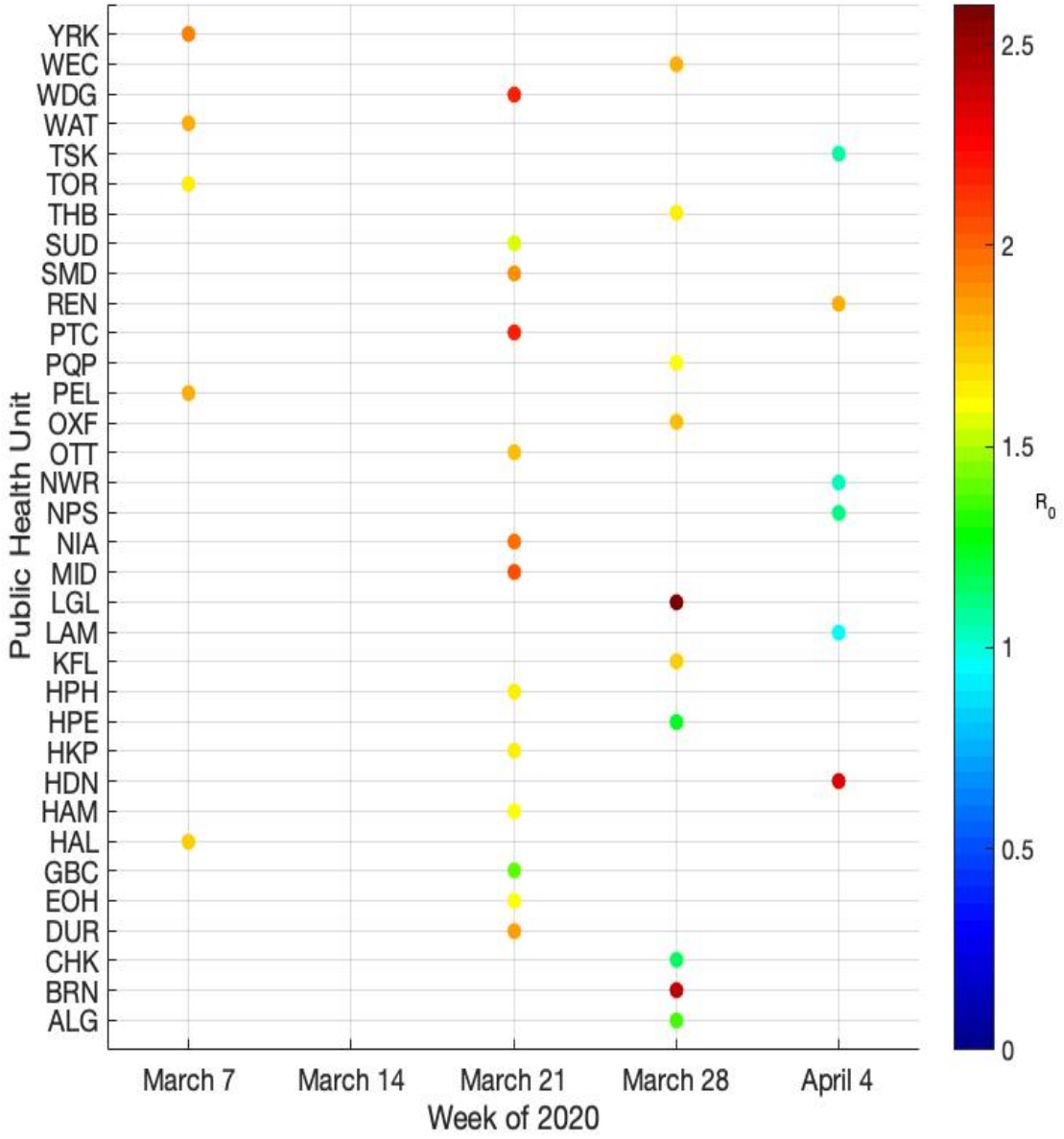

Figure 4.1: R_0 for Ontario's 34 public health units

these reproduction values varying in magnitude from 1.15 to 2.60. In week 5, we determine the remaining 6 PHU R_0 values. We see that the final health units have on average lower R_0 values. Specifically, we see that Haliburton, Kawartha and Pine Ridge District Health Unit, with population density 19.8 $/km^2$, experiences the largest R_0 value and Renfrew Health Unit with (6.9 $/km^2$) experiences a slightly milder R_0 value. Meanwhile, Lambton (42.2

$/km^2$), North Bay and Parry Sound (7.3 $/km^2$), Northwestern (0.4 $/km^2$) and Timiskaming (2.3 $/km^2$) all fall with an R_0 value near 1.

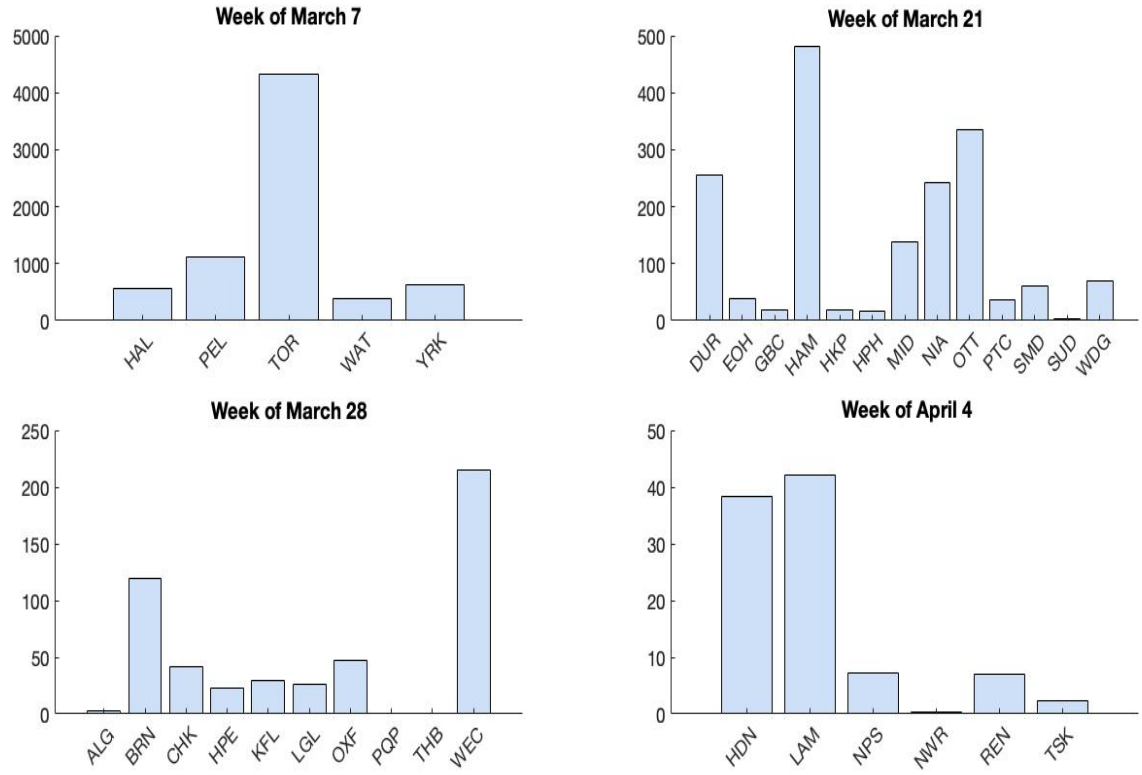

Figure 4.2: Graphs detailing the population density (y-axis) of each PHU (x-axis) for the weeks in which their R_0 values appear in Figure 4.1

While there seemingly is a trend with larger PHUs (population-density wise) and the time in which local infection starts to spread, correlation tests show that there is not a statistically significant relation between the size of R_0 and the specific population density values. This is significant as it has been shown that there is a relationship between population density and the basic reproduction number for a disease [59, 52]. Figure 4.2, exhibits a decrease in overall population density as the weeks progress. Specifically, for the week of March 7^{th}, we see that the population density hovers around 500-1000 $/km^2$. As time progresses, we see the PHU population density decreases within each region. Despite this, we do see regions with lower

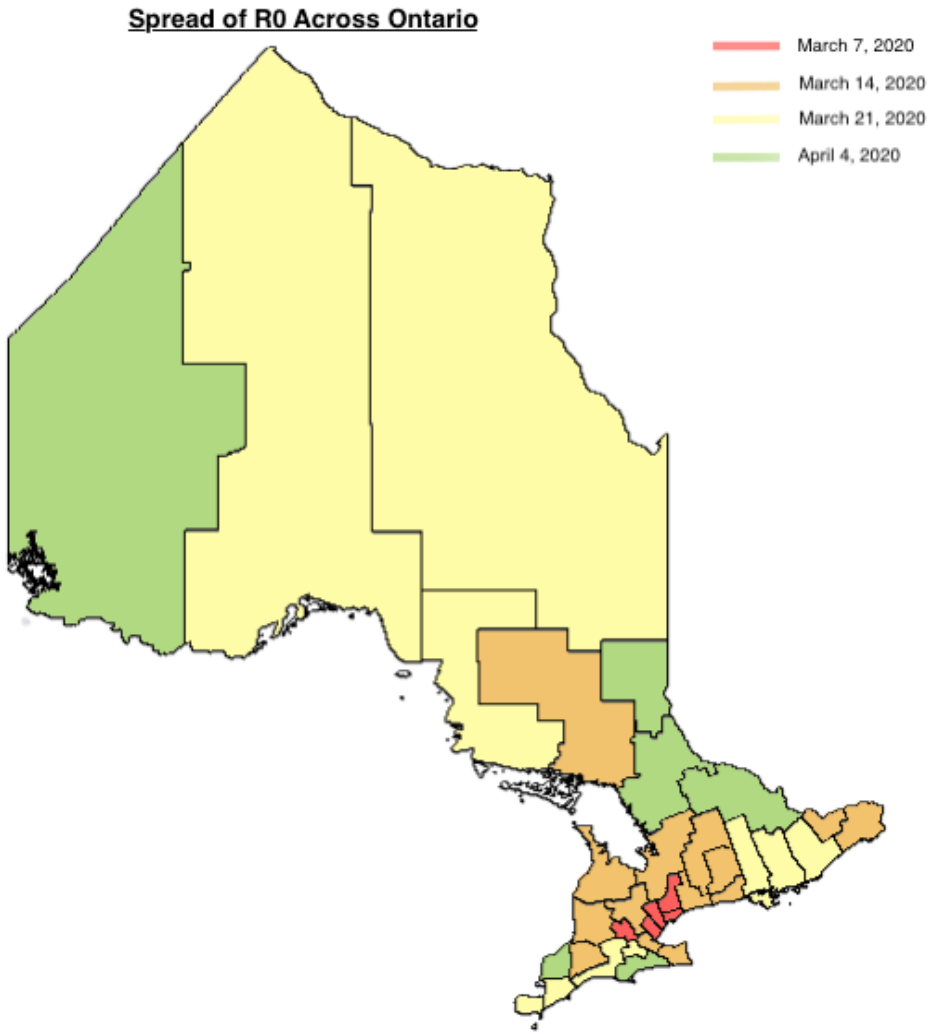

Figure 4.3: Spread of R_0 through the Ontario public health units by the weeks in which the R_0 values were determined.

population densities having these R_0 values begin in the third week in question. While this is perplexing, we note that there is a trend seen in which the initial regions spread infection to their neighboring regions. This may be a result of many things, most likely commuting to work in these larger cities. When we look at Figure 4.3, we can see for Ontario how the COVID-19 disease originated in these large cities and spread outwards to neighboring regions. This provides an interesting insight as we can see there is a spread outwards from these 5 initial health units. As mentioned before, the basic reproduction number is known

to have a relationship with population density however, we seemingly lack this relationship. Having this ability to see how the disease spreads throughout the province demonstrates the possible connection between neighboring PHUs . This idea and possible methods of computation are further discussed in Chapter 5.

4.3 Determining R_{eff} Using Game Results

To obtain the effective reproduction number, recall that R_{eff} can be estimated by the product of basic reproduction number R_0 and the fraction of the total population that is susceptible $s(t)$. Thus, with the expression for $\rho(t)$ determined in 4.7, we can compute $R_{eff_{data}}$ using equation (4.6)

$$R_{eff_{data}}(t) = R_0(\rho)s(t) = R_0(\rho)(1 - c(t)), \text{ where } c(t) = \text{ cumulative incidence} \tag{4.8}$$

Using our expected NPI compliance value from Table 4.1, we follow the same procedure as seen above in Equation 4.8 to determine our effective reproduction number with this game result. While NPI_{comp} is defined by the month, we manipulate the data to correspond to the weeks used to determine $R_{eff_{data}}$. The graph of weekly NPI_{comp} can be seen in Figure 4.4:

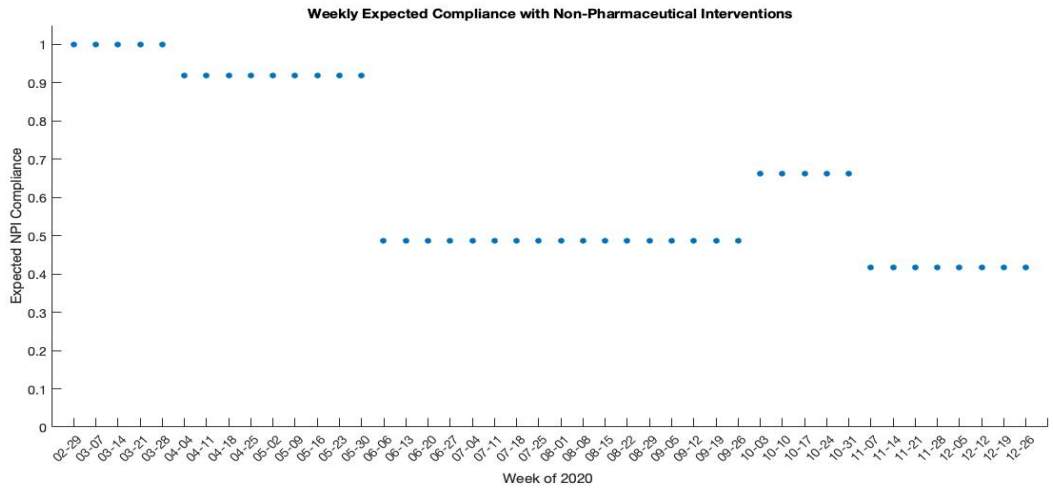

Figure 4.4: Weekly expected NPI compliance over 2020

Meanwhile, the time series of the reproduction number in Ontario, based on incidence data, is in Figure 4.5

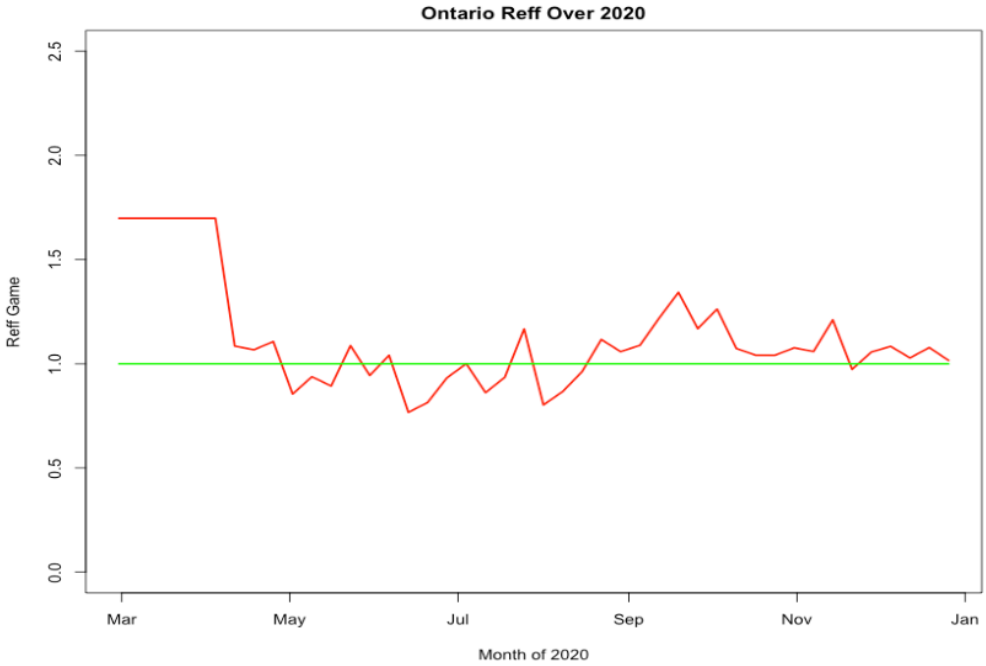

Figure 4.5: Graph of $R_{eff_{data}}$ over the months of interest in 2020

We see that for an assumed level of $eff_{NPI} = 0.5$, the drop in $R_{eff_{data}}$ is accounted for by high levels of expected NPI compliance. When transmission drops, the expected compliance drops also. We depict below several outcomes of expected NPI compliance for a range of values $eff_{NPI} \in [0.2, 0.8]$, to contrast and compare between these and the $R_{eff\,data}$:

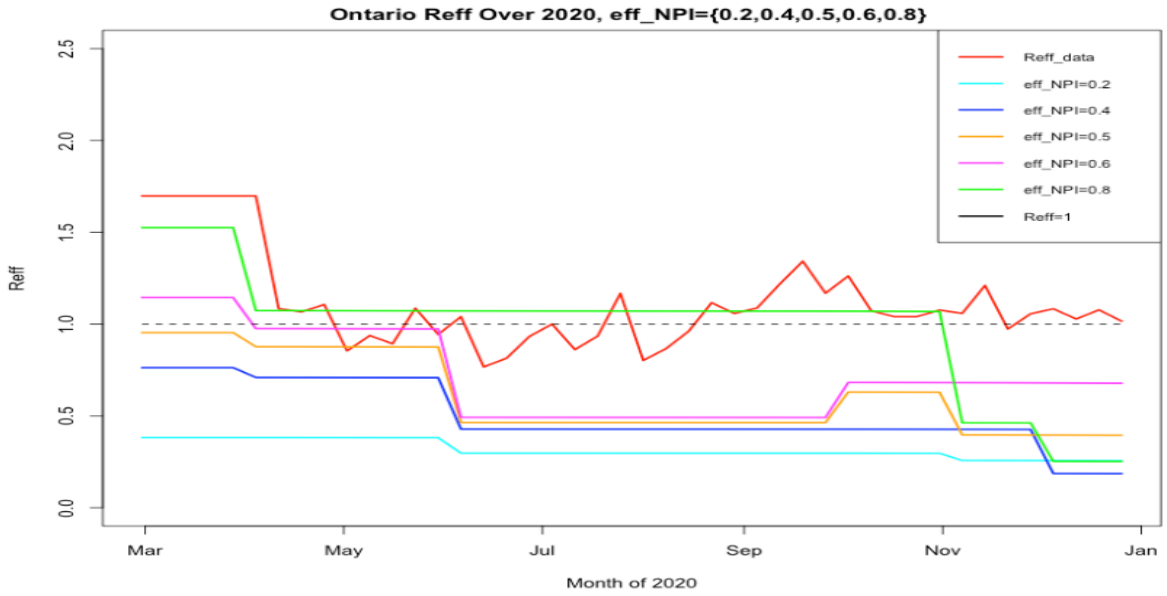

Figure 4.6: Calculated $R_{eff\,game}$ values with different NPI compliance values corresponding to varying $eff_{NPI} \in \{0.2, 0.4, 0.5, 0.6, 0.8\}$

In figure 4.6, we see that a $eff_{NPI} = 20\%$ gives us a step function that continuously decreases as we progressed through 2020. We see a similar curve for $R_{eff\,game}$ when we have an eff_{NPI} value of 40%. The green curve details the case of $eff_{NPI} = 80\%$. This exhibits an initially high $R_{eff\,game}$ with a small decrease which holds over the next several months. Thereafter it quickly drops to a low value of $R_{eff\,game}$ which is when we see the values no longer numerically resemble the curve of $R_{eff\,data}$. The two curves that most closely resemble the behaviour of $R_{eff\,data}$ are those with $eff_{NPI} = 0.5$ and $eff_{NPI} = 0.6$. While an eff_{NPI} value of 60% behaves similarly to that of $eff_{NPI} = 0.5$, we do not see a decrease in expected NPI compliance in the last months which is shown in $R_{eff\,data}$. Thus, we can see that while an eff_{NPI} value of 50% has the most similar plot to that of $R_{eff\,data}$, the curve of $R_{eff\,game}$

with $eff_{NPI} = 80\%$ provides us with the most accurate numerical values for the months of March to October 2020. To further expand upon this work, in Chapter 5 we discuss the case of a time-varying function for eff_{NPI} and the possibilities it holds for future work.

4.3.1 Analysing R_0 and $R_{effdata}$

Similar to the analyses done in Chapter 2, we look to investigate the possible relationships existing between the 34 basic reproduction numbers and what effect they have on transmission potential. The variables of interest are those discussed in Chapter 2: median age [7], median income [7], average temperature of the PHU and the proportion of population with post-secondary education [7]. By performing this correlation analysis, we found that there are some variables that appear to have a correlation while other showed less correlation. These results are highlighted in Figure 2.1 and discussed below:

We can see here that the proportion of the population with post secondary education and the density of the population have correlation coefficients very close to zero. While the former is not of significant interest, the latter poses a perplexing case of no correlation between population density of a region and the basic reproduction number of a disease. As we are looking at the case where we have no interventions of any sort, we know that this lack of a relationship cannot be due to COVID-19 and NPI fatigue. However, as we are looking at the case where individuals were still going to work, there are aspects such as commuters and travellers that are not accounted for. Moreover, as shown in Figure 4.3, we see that the basic reproduction numbers spread throughout the province after a neighboring region experiences the first initial increase in cases. Therefore it is possible that R_0 across these 34 regions does not necessarily depend upon the density of that region but rather what is happening in neighboring regions.

The two variables that seemingly have stronger relationships are that of median income

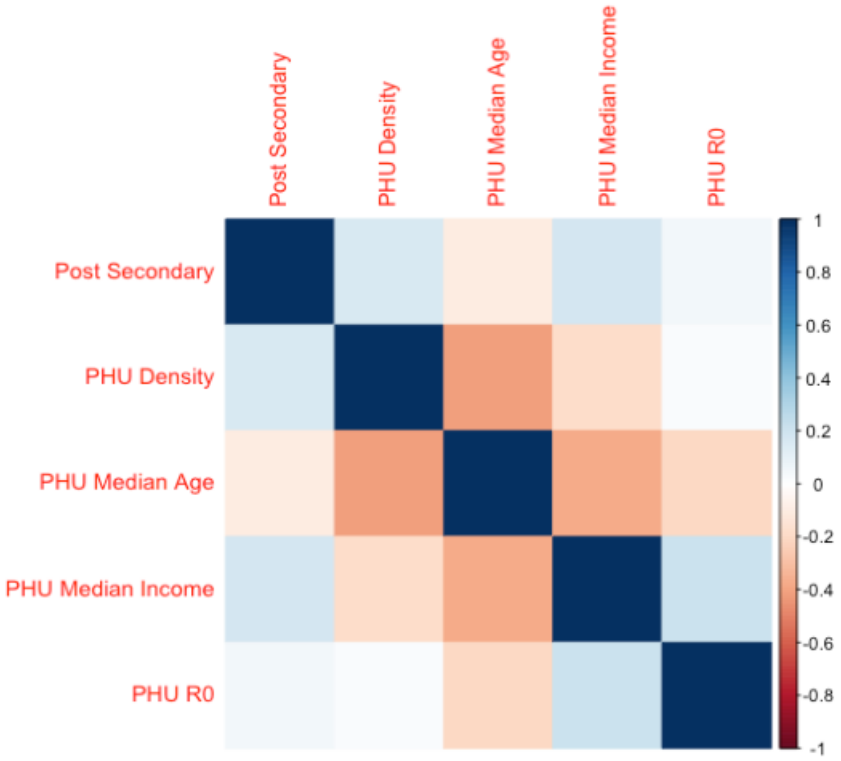

Figure 4.7: Correlation matrix for parameters of interest and R_0 across each of the 34 public health units

and median age. For median income we see a positive correlation to the basic reproduction number. As discussed in Chapter 2, this relationship is most likely due to the fact that regions with lower median income most likely host more essential workers. As such, those regions with higher incomes host more workers that were able to work from home or avoid close contact with the general public. Moreover, we see a negative correlation between median age and R_0. This negative relationship can be attributed to the fact that regions with lower median age host younger individuals who are more likely to go out and interact with the general public. As such, they are exposed to more people, increasing their risk of infection and thus the basic reproduction number of a region.

Chapter 5

Conclusion

5.1 Discussion of Results

The aim of this thesis was to develop a way to describe disease transmission on a more granular scale across Ontario. Within Chapter 2, we determined and described the perceived risk of infection and personal discomfort of NPI compliance. Across the 34 health units, we determined these monthly risk and discomfort parameters using data analytics and statistical methods. We had to manipulate certain aspects of the case data to determine the daily cases, deaths and scaled daily change at the PHU level. We categorized the provincial mask compliance, stringency index and hospitalizations to be able to use in our regression analysis. Finally, we worked with the Google Mobility data to get it from census divisions to public health units. With these values we were able to see how risk and discomfort factors changed throughout the year and amongst health units. These values allowed us to determine the Nash equilibrium across Ontario, giving us a PHU's probability of respecting NPIs for some month. Additionally we determine the expected NPI compliance for Ontario using these Nash equilibria. Furthermore, we investigate the relationship between $R_{eff\,data}$ and the expected NPI compliance of various NPI efficacy values. With these results we found

an assumed NPI efficacy of 50% provides us with the most similar behaviour exhibited in the figure of $R_{eff\,data}$ 4.5. We also determined and plotted the R_0 values determined for each PHU which provided insight into the transmission potential of COVID-19. These results are highlighted in figures 4.1 and 4.3.

Throughout this thesis we saw a common theme of population density not playing the typical role seen in disease transmission [52]. Specifically, in the months where there was a statistically significant relation between population density and perceived risk of infection $\bar{r}$ or personal discomfort factor $\tilde{r}$, we saw a negative correlation between these variables. Recall that we can attribute these negative correlations to NPI and COVID-19 fatigue experienced by individuals in densely populated regions. Moreover, for the basic reproduction number, we found that there was no correlation with population density. These counterintuitive results provide fascinating takeaways as we note the possible relationship between neighboring PHUs.

For the majority of the work done in this thesis, we used the publicly available software R. For determining our perceived risk and personal discomfort factors, R proved to be extremely useful and well adept to manipulating the data to be in a usable format. Additionally, R performed very well in the determination of our R_0 and $R_{eff\,game}$. We encountered some issues however when performing the optimization. R could not perform the type of optimization we wished to use despite multiple efforts using various optimization solvers. We instead used MATLAB, or the publicly available version OCTAVE, and made use of the general optimization solver SOLNP. An additional limitation we encountered while using R is that of plotting with colour as a third dimension, specifically in reference to Figure 4.1. It was much easier to plot this figure in MATLAB as they have a color-bar feature that is much easier to work with. Despite the issues faced when using R, the software overall was sufficient for the computational needs of this thesis. We achieved our goal of describing perceived risks of infection and personal discomfort of NPI compliance at the PHU level. Additionally, we

showed that this granular view across the 34 PHUs can provide helpful insight to expected NPI compliance for the province. Moreover, the R_0 values for each PHU provide us with a visual example of how the basic reproduction numbers came up throughout the province.

5.2 Limitations and Future Work

While the work done in this thesis looked to describe a more granular view of the interconnectedness between Ontario's PHUs under the lens of the COVID-19 pandemic, we experienced a number of limitations in our calculations. Within our determination of the risk parameters in Chapter 2, we assumed that the Y-values in our regression are independent, that they can be expressed as a linear function of our dependent variables, the variation around the regression line is constant and for any given values of X, the Y values are normally distributed. Additionally, we encounter the issue of Google not sharing the precise methodologies for their calculations of social mobility scores. In future work, further insight into how they perform these computations could reduce some ambiguity associated with the model. Moreover, within our model we made the assumption that all players within a region will adopt the same perceived risk of infection and personal discomfort factor. Future work could look to further refine this work to age groups with PHUs to minimize the effect this assumption has.

As mentioned in Chapter 3, we did not have the same research and data available for COVID-19 disease spread. Consequently, we were unable to use the same methods for determining the perceived probability of becoming infected π_p and thus we had to make a simplification to better suit the COVID-19 lens. Additionally, we assume that the perceived effect NPIs have on deterring further disease transmission across Ontario is 50%. As this perceived effect changes, this leads to varying expected NPI compliance measures. As such, these changes result in varying effective reproduction numbers.

As we are looking at regions with interacting populations, there is the possibility of spatial dependence in the data. This can be problematic when we are using our regression methods as they do not account for spatial variation as a relationship within the model [13]. For an ordinary least squares estimation of the regression model, we assume that the coefficients of the explanatory variable Y are constant across the space in question. If however there is spatial dependence in the data, these assumptions are violated. In such a case, we would need to implement a spatial regression model. In our pursuit of determining the risk parameters, we investigate the possibility of spatial regression. In this pursuit, we encountered issues obtaining appropriate data corresponding to Ontario's public health boundaries to satisfy the requirements of the computational model. The proper implementation of spatial regression may provide further insight into the transmission and relationship between regions and thus, is a valuable avenue to further investigate. Furthermore, in this thesis we focus on the spread of disease amongst PHUs over 2020. While this provides valuable insight into the dynamics in the beginning of the pandemic, it does not address the more complex, but interesting case of 2021 where we had vaccine rollouts throughout the year as well as extreme NPI fatigue. Further analyses accounting for these extra factors could provided valuable information as to how disease transmission and NPI compliance changed over the course of the pandemic.

5.3 Concluding remarks

In this thesis we illustrate the dynamics of disease transmission among Ontario's 34 public health regions with the use of NPIs. We formulate a model of perceived risk of infection and personal discomfort of complying with NPIs specific to Ontario's 34 PHUs . With this we are able to see at a refined level how human behaviour impacts disease transmission. Furthermore, with the correlation analysis performed in Chapter 2, we obtain a better idea of what factors have a statistically significant relationship with our risk parameters. With

these results, health care systems can evaluate what possible trends may lead to an increase or decrease in risk parameters and act accordingly to help mitigate the spread of a disease.

Through the use of our game theoretic approach we are able to determine the probability that a given player from one of Ontario's PHUs respects non-pharmaceutical measures across the time frame of interest. Consequently, we obtain the expected NPI compliance within Ontario across the ten months of interest. These expected NPI compliance rates follow the trends seen in $R_{eff\,data}$ and suggest that we have an appropriately fitting model of NPI compliance across Ontario. Through the use of daily case data, we are able to determine each PHUs basic reproduction number before the implementation of any NPIs. As such, we are able to visualize how the disease spreads across the province using Figure 4.3 as well as the severity of the R_0 value using Figure 4.2. Having this ability to see how the disease spreads around the province is extremely useful as it may provides insight to transmission dynamics which health care officials could use for preventative measures. Therefore, while this model is tailored to the COVID-19 pandemic, with minor adjustments and appropriate data, one could extend this to any virus or disease that may be of concern.

REFERENCES

[1] Confirmed positive cases of COVID-19 in Ontario - Datasets - Ontario Data Catalogue.

[2] COVID-19 cases in hospital and ICU, by Ontario Health (OH) region - Datasets - Ontario Data Catalogue.

[3] COVID-19 Map - Johns Hopkins Coronavirus Resource Center.

[4] Google COVID-19 Community Mobility Reports.

[5] Nonpharmaceutical Interventions (NPIs) — CDC.

[6] WHO Coronavirus (COVID-19) Dashboard — WHO Coronavirus (COVID-19) Dashboard With Vaccination Data.

[7] 2016 Census Profile.

[8] COVID-19 cases, hospitalizations and deaths in Ontario — CTV News, March 2020.

[9] COVID-19 Response Framework: Keeping Ontario Safe and Open —Lockdown Measures.

[10] COVID-19 – What We Know So Far About... Asymptomatic Infection and Asymptomatic Transmission.

[11] Table 22-10-0143-01 Smartphone personal use and selected smartphone habits by gender and age group, June 2021.

[12] Public Health Units - Health Services in Your Community - MOHLTC, March 2021.

[13] Anselin, L. Spatial regression. *The SAGE handbook of spatial analysis 1* (2009), 255–276.

[14] Bauch, C. T., and Earn, D. J. Vaccination and the theory of games. *Proceedings of the National Academy of Sciences 101*, 36 (2004), 13391–13394.

[15] Brauer, F. *Mathematical Biosciences*.

[16] Ceci, L. Top U.S. mapping apps by downloads 2021, February 2022.

[17] Cheung, C., Lyons, J., Madsen, B., Miller, S., and Sheikh, S. The Bank of Canada COVID-19 stringency index: measuring policy response across provinces.

[18] Cojocaru, M., and Jonker, L. Projected differential equations in Hilbert spaces. *Proc. Amer. Math. Soc 132*, 1 (2004), 183–193.

[19] Cojocaru, M. G., Athar, S., and Thommes, E. W. Adoption costs of new vaccines - A Stackelberg dynamic game with risk-perception transition states. *Infectious Disease Modelling 3* (jan 2018), 256–265.

[20] Cojocaru, M. G., Bauch, C. T., and Johnston, M. D. Dynamics of vaccination strategies via projected dynamical systems. *Bulletin of Mathematical Biology 69*, 5 (2007), 1453–1476.

[21] Coronaviridae Study Group of the International Committee on Taxonomy of Viruses. Nonpharmaceutical Interventions (NPIs) — CDC.

[22] Division, P. A. Compliance with Mask. Tech. rep., 2020.

[23] Fields, R., Humphrey, L., Flynn-Primrose, D., Mohammadi, Z., Nahirniak, M., Thommes, E. W., and Cojocaru, M. G. Age-stratified transmission model of COVID-19 in Ontario with human mobility during pandemic's first wave. *Heliyon 7*, 9 (September 2021).

[24] Freedman, D. A. *Statistical models: theory and practice*. cambridge university press, 2009.

[25] Hale, T., Anania, J., Angrist, N., Boby, T., Cameron-Blake, E., Di, M., Lucy, F., Goldszmidt, E. R., Hallas, L., Kira, B., Luciano, M., Majumdar, S., Nagesh, R., Petherick, A., Phillips, T., Tatlow, H., Webster, S., Wood, A., and Zhang, Y. Variation in government responses to COVID-19.

[26] Harrison, A. G., Lin, T., and Wang, P. *Trends in Immunology*.

[27] He, W., Yi, G. Y., and Zhu, Y. *Journal of medical virology*.

[28] Heesterbeek, J., et al. On the definition and the computation of the basic reproduction ratio r_0 in models for infectious diseases in heterogeneous populations. *Journal of mathematical biology 28* (1990), 365.

[29] Humphrey, L., Thommes, E. W., Fields, R., Coudeville, L., Hakim, N., Chit, A., Wu, J., and Cojocaru, M. G. Large-scale frequent testing and tracing to supplement control of Covid-19 and vaccination rollout constrained by supply. *Infectious Disease Modelling 6* (Jaurary 2021), 955–974.

[30] Humphrey, L., Thommes, E. W., Fields, R., Hakim, N., Chit, A., and Cojocaru, M. G. A path out of COVID-19 quarantine: an analysis of policy scenarios. *medRxiv* (April 2020), 2020.04.23.20077503.

[31] Liu, Y., Gayle, A. A., Wilder-Smith, A., and Rocklöv, J. The reproductive number of COVID-19 is higher compared to SARS coronavirus. *Journal of Travel Medicine 2020* (2020), 1–4.

[32] Ma, J. Estimating epidemic exponential growth rate and basic reproduction number. *Infectious Disease Modelling 5* (Jaurary 2020), 129–141.

[33] Mizumoto, K., Kagaya, K., Zarebski, A., and Chowell, G. Estimating the asymptomatic proportion of coronavirus disease 2019 (COVID-19) cases on board the Diamond Princess cruise ship, Yokohama, Japan, 2020. *Eurosurveillance 25*, 10 (March 2020), 2000180.

[34] Mohammadi, Z., Cojocaru, M. G., and Thommes, E. W. Human behaviour , NPI and mobility reduction effects on COVID-19 transmission in different countries of the world.

[35] Munger, A. 2016 CENSUS HIGHLIGHTS: Factsheet 14, February 2018.

[36] Myerson, R. B. *Game theory: analysis of con ict*. Harvard university press, 1997.

[37] Nagurney, A., and Siokos, S. *Financial networks : statics and dynamics*. Berlin, 1997.

[38] Nash, J. F., et al. Equilibrium points in n-person games. *Proceedings of the national academy of sciences 36*, 1 (1950), 48–49.

[39] O'Connor, C., November, title = Regulations Released: Adjusting to Ontario's Colour-Coded COVID-19 Zones, url = https://hicksmorley.com/2020/11/11/adjusting-to-ontarios-new-colour-coded-covid-19-zones/, urldate = 2022-02-01, year = 2020.

[40] of the International, C. S. G., et al. The species severe acute respiratory syndrome-related coronavirus: classifying 2019-ncov and naming it sars-cov-2. *Nature microbiology 5*, 4 (2020), 536.

[41] Office of the Premier, December, title = Ontario Announces Provincewide Shutdown to Stop Spread of COVID-19 and Save Lives — Ontario Newsroom, url = https://news.ontario.ca/en/release/59790/ontario-announces-provincewide-shutdown-to-stop-spread-of-covid-19-and-save-lives, urldate = 2022-02-01, year = 2020.

[42] Office of the Premier. Ontario Enacts Provincial Emergency and Stay-at-Home Order — Ontario Newsroom, April 2021.

[43] Office of the Premier. Ontario Releases Three-Step Roadmap to Safely Reopen the Province, May 2021.

[44] Osborne, M. J., and Rubinstein, A. *A Course in Game Theory*. The MIT Press, Cambridge, Massachusetts, 1994.

[45] Phillips, T., and Tatlow, H. Codebook for the Oxford Covid-19 Government Response Tracker, Jaurary 2022.

[46] Pringle, J. Ottawa breaks record for most COVID-19 cases with 194 on New Year's Eve: Public Health Ontario — CTV News, 2020.

[47] Salomon, J. A., Reinhart, A., Bilinski, A., Chua, E. J., la Motte-Kerr, W., Rönn, M. M., Reitsma, M. B., Morris, K. A., LaRocca, S., Farag, T. H., Kreuter, F., Rosenfeld, R., and Tibshirani, R. J. *Proceedings of the National Academy of Sciences of the United States of America*.

[48] Schneider, A., Hommel, G., and Blettner, M. *Deutsches Arzteblatt*.

[49] Stevens, N. T., Kiwon, F., and Steiner, S. H. Estimating the Effects of Non-Pharmaceutical Interventions (NPIs) and Population Mobility on Daily COVID-19 Cases: Evidence from Ontario. 2021–2043.

[50] Stoer, J., and Bulirsch, R. *Introduction to Numerical Analysis*, 3 ed. Springer, New York, 2002.

[51] Stutt, R. O., Retkute, R., Bradley, M., Gilligan, C. A., and Colvin, J. A modelling framework to assess the likely effectiveness of facemasks in combination with lock-down in managing the COVID-19 pandemic. *Proceedings of the Royal Society A 476*, 2238 (2020).

[52] Sy, K. T. L., White, L. F., and Nichols, B. E. Population density and basic reproductive number of COVID-19 across United States counties. *PLOS ONE 16*, 4 (April 2021), e0249271.

[53] Tuite, A. R., Fisman, D. N., and Greer, A. L. Mathematical modelling of COVID-19 transmission and mitigation strategies in the population of Ontario, Canada. *CMAJ 192*, 19 (May 2020), E497–E505.

[54] Van den Driessche, P. Reproduction numbers of infectious disease models. *Infectious Disease Modelling 2*, 3 (August 2017), 288–303.

[55] Van den Driessche, P., and Watmough, J. Further notes on the basic reproduction number. *Mathematical epidemiology* (2008), 159–178.

[56] WHO. Tech. rep., World Health Organization, January.

[57] Wilson, A. M., Abney, S. E., King, M. F., Weir, M. H., López-García, M., Sexton, J. D., Dancer, S. J., Proctor, J., Noakes, C. J., and Reynolds, K. A. COVID-19 and use of non-traditional masks: how do various materials compare in reducing the risk of infection for mask wearers? *The Journal of Hospital Infection 105*, 4 (August 2020), 640.

[58] Wimmer, E., and Goldbach, R. Viral Genetics. *Current Opinion in Genetics and Development 2*, 1 (1996), 59–60.

[59] Wong, D. W., and Li, Y. *PLOS ONE*.

[60] Wu, J., Tang, B., Bragazzi, N. L., Nah, K., and McCarthy, Z. *Journal of mathematics in industry*.

[61] Ye, Y. SOLNP USERS' GUIDE. Tech. rep., Stanford University.

[62] ZARANTONELLO, E. H. Projections on Convex Sets in Hilbert Space and Spectral Theory: Part I. Projections on Convex Sets: Part II. Spectral Theory. In *Contributions to Nonlinear Functional Analysis*, E. H. Zarantonello, Ed. Academic Press, 1971, pp. 237–424.

[63] Zhou, P., Yang, X. L., Wang, X. G., Hu, B., Zhang, L., Zhang, W., Si, H. R., Zhu, Y., Li, B., Huang, C. L., Chen, H. D., Chen, J., Luo, Y., Guo, H., Jiang, R. D., Liu, M. Q., Chen, Y., Shen, X. R., Wang, X., Zheng, X. S., Zhao, K., Chen, Q. J., Deng, F., Liu, L. L., Yan, B., Zhan, F. X., Wang, Y. Y., Xiao, G. F., and Shi, Z. L. A pneumonia outbreak associated with a new coronavirus of probable bat origin. *Nature 579*, 7798 (2020), 270–273.

APPENDIX

Appendix A

Supplementary explanation for Bank of Canada Stringency Index

The Bank of Canada (BoC) adapted the OxCGRT stringency index to create a stringency index of their own which is a measure of containment policies and public information campaigns [17]. More specifically, this index focuses on the economic impact of COVID-19. Similar to the OxCGRT, the BoC's stringency index does not measure the efficacy of a province's response to COVID-19 nor does it provide a direct measure of the impact of government policies on the economy [17]. As of the summer 2020, researchers have been collecting publicly available information on government policies, creating daily government response indexes for all 10 provinces. With this, the bank could systematically measure, track and compare government policy responses. The BoC's stringency index follows the methodology of the OxCGRT with a few adjustments to make it more appropriate for the Canadian context and to capture specific differences in policy responses. In the BoC's stringency index, they added 3 policy indicators to the OxCGRT stringency index which included the following

- $C9$ - Restrictions on inter-provincial travel which splits the original OxCGRTs "internal

movement restrictions" ($C7$) to capture only intra-provincial travel. Therefore adding this new $C9$ term gives greater weight to travel restrictions in the stringency index

- $C10$ - Enforcement mechanisms for individuals: OxCGRT does not include a measure identifying differences in provinces that have similar containment policies but different punishments or enforcement of these policies. This C10 indicator captures penalties for individuals violating public health orders

- $C11$ - Enforcement mechanisms for businesses violating public health orders

By adding more targeted dimensions, they increase the level of detail in the variation across provinces as well as over time. Additional geographical dimensions were included in the BoC index including types of outdoor events, outdoor versus indoor events and exceptions for certain travellers. Additionally, they refined the categories of coding values for several policy indicators based on a more detailed examination of policies in Canada. While they added categories to their indicators, the sub-index calculation decreases as the denominator in this equation increases

$$Sub - Index_j = 100 \times \left(\frac{a_j - \sum_{i=1}^{n} (\frac{1 \quad f_{ij}}{n+1})}{b_j} \right) \tag{A.1}$$

- a_j is the ordinal value for the most restrictive measures in place within the province

- b_j is the maximum coding value

- n_j is the total number of targeting dimensions (e.g., by geography)

- f_{ij} is the flag for targeting dimension, i, which is equal to 1 if the policy is general or 0 if targeted

As a result of this increasing b term, often the sub-index is lower when compared with OxCGRT. While the BoC stringency index is better tailored to the Canadian landscape and

the resulting economic implications, it does not provide a more refined scale and thus we still only have provincial data. Additionally, these factors which cater to the economic side of the stringency measures do not help us better fit our model to describe the behaviour of individuals in a given PHU. Thus we use the broader scope of the OxCGRT stringency index in our determination of the risk parameters.